Received: 10 February 2018 | Revised: 19 July 2018 | Accepted: 3 August 2018

DOI: 10.1111/avsc.12401

SYNTHESIS

Applied Vegetation Science IAVS

Vegetation on mesic loamy and sandy soils along a 1700-km maritime Eurasia Arctic Transect

Donald A. Walker[1] | Howard E. Epstein[2] | Jozef Šibík[3] | Uma Bhatt[4] | Vladimir E. Romanovsky[4] | Amy L. Breen[5] | Silvia Chasníková[3] | Ronald Daanen[6] | Lisa A. Druckenmiller[1] | Ksenia Ermokhina[7,8] | Bruce C. Forbes[9] | Gerald V. Frost[10] | Jozsef Geml[11] | Elina Kaärlejarvi[12] | Olga Khitun[13] | Artem Khomutov[14] | Timo Kumpula[15] | Patrick Kuss[16] | Georgy Matyshak[17] | Natalya Moskalenko[7] | Pavel Orekhov[7] | Jana Peirce[1] | Martha K. Raynolds[1] | Ina Timling[1]

[1]Alaska Geobotany Center, Institute of Arctic Biology & Department of Biology and Wildlife, University of Alaska, Fairbanks, Alaska

[2]Department of Environmental Sciences, University of Virginia, Charlottesville, Virginia

[3]Plant Science and Biodiversity Center, Slovak Academy of Sciences, Institute of Botany, Bratislava, Slovak Republic

[4]Geophysical Institute & Department of Atmospheric Science, University of Alaska, Fairbanks, Alaska

[5]International Arctic Research Center, University of Alaska, Fairbanks, Alaska

[6]Division of Geological & Geophysical Surveys, Fairbanks, Alaska

[7]Earth Cryosphere Institute, Tyumen Scientific Center, Russian Academy of Sciences, Siberian Branch, Tyumen, Russia

[8]A.N. Severtsov Institute of Ecology and Evolution Russian Academy of Science, Moscow, Russia

[9]Arctic Center, University of Lapland, Rovaniemi, Finland

[10]Alaska Biological Research, Inc., Fairbanks, Alaska

[11]Naturalis Biodiversity Center, CR Leiden, The Netherlands

[12]Department of Ecology and Environmental Sciences, Umeå University, Umeå, Sweden

[13]Komarov Botanical Institute, Russian Academy of Sciences, St. Petersburg, Russia

[14]University of Tyumen, Tyumen, Russia

[15]University of Eastern Finland, Joensuu, Finland

[16]Institute of Systematic and Evolutionary Botany, University of Zürich, Zürich, Switzerland

[17]Department of Soil Science, Lomonosov Moscow State University, Moscow, Russia

Correspondence
Donald A. Walker, Alaska Geobotany Center, Institute of Arctic Biology & Department of Biology and Wildlife, University of Alaska, Fairbanks, AK.
Email: dawalker@alaska.edu

Funding information
U.S. National Science Foundation, Arctic Science Engineering and Education for Sustainability Program, Grant/Award Number: 1263854; Russia Academy of Science; Bureau of Ocean Energy

Abstract

Questions: How do plant communities on zonal loamy vs. sandy soils vary across the full maritime Arctic bioclimate gradient? How are plant communities of these areas related to existing vegetation units of the European Vegetation Classification? What are the main environmental factors controlling transitions of vegetation along the bioclimate gradient?

Location: 1700-km Eurasia Arctic Transect (EAT), Yamal Peninsula and Franz Josef Land (FJL), Russia.

Nomenclature: Pan-Arctic Species List (PASL) (Raynolds et al., 2013), a circumpolar compendium of accepted names for vascular plants (Elven, Murray, Razzhivin, & Yurtsev, 2011), mosses (Belland et al., 2012), liverworts (Konstantinova & Bakalin, 2009) and lichens (Kristinsson, Hansen, & Zhurbenko, 2010).

Management (BOEM); Slovak Academy of Science, Grant/Award Number: 2/0135/1; U.S. National Aeronautics and Space Administration, Land-Cover Land-Use Change Program, Grant/Award Number: NNG6GE00A, NNX09AK56J and NNX14AD90G

Co-ordinating Editor: Borja Jiménez-Alfaro

Methods: The Braun-Blanquet approach was used to sample mesic loamy and sandy plots on 14 total study sites at six locations, one in each of the five Arctic bioclimate subzones and the forest–tundra transition. Trends in soil factors, cover of plant growth forms (PGFs) and species diversity were examined along the summer warmth index (SWI) gradient and on loamy and sandy soils. Classification and ordination were used to group the plots and to test relationships between vegetation and environmental factors.

Results: Clear, mostly non-linear, trends occurred for soil factors, vegetation structure and species diversity along the climate gradient. Cluster analysis revealed seven groups with clear relationships to subzone and soil texture. Clusters at the ends of the bioclimate gradient (forest–tundra and polar desert) had many highly diagnostic taxa, whereas clusters from the Yamal Peninsula had only a few. Axis 1 of a DCA was strongly correlated with latitude and summer warmth; Axis 2 was strongly correlated with soil moisture, percentage sand and landscape age.

Conclusions: Summer temperature and soil texture have clear effects on tundra canopy structure and species composition, with consequences for ecosystem properties. Each layer of the plant canopy has a distinct region of peak abundance along the bioclimate gradient. The major vegetation types are weakly aligned with described classes of the European Vegetation Checklist, indicating a continuous floristic gradient rather than distinct subzone regions. The study provides ground-based vegetation data for satellite-based interpretations of the western maritime Eurasian Arctic, and the first vegetation data from Hayes Island, Franz Josef Land, which is strongly separated geographically and floristically from the rest of the gradient and most susceptible to on-going climate change.

KEYWORDS

above-ground biomass ordination, Arctic, bioclimate subzones, Braun-Blanquet classification, DCA ordination, Normalized Difference Vegetation Index, plant growth forms, remote sensing, soil texture, summer warmth index, tundra biome

1 | INTRODUCTION

Arctic tundra ecosystems occur in a broad circumpolar belt that extends from areas north of 80°N to forest–tundra areas south of 60°N, with mean July temperatures that vary from near 0°C to over 12°C. Several conceptual approaches have been used to subdivide the vegetation along the broad bioclimate gradients of Eurasia (Alexandrova, 1980; Chernov & Matveyeva, 1997; Yurtsev, 1994a), North America (Bliss, 1997; Daniëls, Bültmann, Lünterbusch, & Wilhelm, 2000; Edlund, 1990; Polunin, 1951) and the circumpolar Arctic (Elvebakk, Elven, & Razzhivin, 1999; Tuhkanen, 1984; Walker et al., 2005; Yurtsev, 1994b). Only a few studies, however, have attempted to examine continuous vegetation transitions of zonal plant communities along transects that traverse the full Arctic bioclimate gradient because of the rather daunting logistics involved. Examples exist for the Taymyr Peninsula, Russia (Matveyeva, 1998), the North America Arctic Transect (NAAT; Walker, Kuss, et al., 2011) and the 1999 Canada transect for the Circumpolar Arctic Vegetation Map (Gonzalez, Gould, & Raynolds, 2000). Arctic alpine vegetation gradients have been described along elevation gradients in the mountains of southwest Greenland (Sieg, Drees, & Daniëls, 2006).

Here we describe the vegetation along the 1700-km Eurasia Arctic Transect (EAT) that includes the Yamal Peninsula and Franz Josef Land (Figure 1). The aim is to characterize vegetation on zonal loamy and sandy soils along the complete maritime Arctic climate gradient in western arctic Russia to aid in remote-sensing interpretations of land-cover and land-use change (Walker, Epstein, et al., 2012). The zonal patterns, geological conditions, permafrost and summer thaw depth (active layer) conditions are generally well described along the length of the peninsula. We analyse the variations in plant growth forms and species richness in each layer of the plant canopy with respect to summer temperature and soil texture, present a preliminary numerical classification and use indirect ordination methods to analyse the relationship of the plots and species to a suite of measured environmental factors.

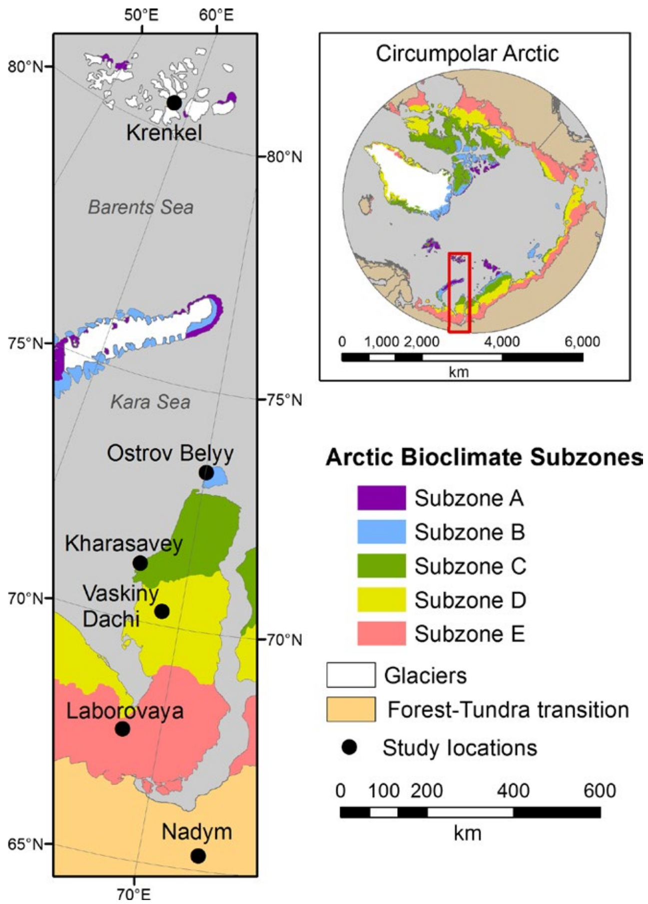

FIGURE 1 The Eurasia Arctic Transect and Arctic bioclimate subzones. Inset map shows circumpolar distribution of the subzones according to the Circumpolar Arctic Vegetation Map (CAVM Team et al., 2003)

2 | METHODS

2.1 | Site selection and sampling

We established the EAT during four expeditions in the summers of 2007–2010 (Figure 1). The transect extends from the Krenkel Hydro-meteorological Station on Hayes Island (80°37′N, 58°03′E) in the maritime polar desert of Franz Josef Land, to Nadym (65°19′N, 72°53′E) in the forest–tundra transition of west Siberia. Mean July temperatures range from 1°C at the northern end of the transect to 15.8°C at the southern end. Six study locations were selected along the EAT to represent zonal (Razzhivin, 1999; Walter, 1954, 1973) vegetation conditions in each of the five Arctic bioclimate subzones and the forest–tundra transition, as mapped on the Circumpolar Arctic Vegetation Map (Walker et al., 2005; Yurtsev, 1994b; Table 1). At each location we chose at least two study sites — one on mesic loamy soils and one on mesic sandy soils (see Supporting Information Appendix S1 for geological setting in relationship to soils).

We used the Braun-Blanquet approach (Westhoff & Van der Maarel, 1978) to sample mesic loamy and sandy sites at each location. At most study sites there was adequate space for a large relatively homogeneous 50 m × 50 m sample site that corresponded approximately to the 30-m to 70-m pixel size of the Landsat satellite sensors. Sample plots and transects were arranged in the pattern shown in Supporting Information Appendix S2. Here we describe the data mainly from 5 m × 5 m (25 m^2) plots, except at the Nadym forest site, where 10 m × 10 m (100 m^2) plots were used, and the Nadym tundra site, where 1 m × 1 m (1 m^2) plots were used to sample homogeneous areas of vegetation on patterned ground features (earth hummocks). We sampled 79 plots, but eliminated three Nadym wetland plots, resulting in a final data set of 76 plots, distributed among the six EAT locations: Krenkel (KR, ten plots), Ostrov Belyy (BO, 20 plots), Laborovaya (LA, ten plots), Kharasavey (KH, ten plots), Vaskiny Dachi (VD, 15 plots) and Nadym (ND, 11 plots) (see Supporting Information Appendix S3 for descriptions and photographs of the study sites.)

Each vascular plant, bryophyte and lichen species occurring within a plot was recorded and a sample taken as a voucher. Unknown species were sent to the Komarov Botanical Institute (KBI) for final identification. The cover-abundance of each species was recorded using Braun-Blanquet categories (*r* = single occurrence; + = several occurrences but <1% cover; 1 = 1%–5% cover; 2 = 6%–25%; 3 = 26%–50%; 4 = 51%–75%; 5 = 76%–100%; Braun-Blanquet, 1928). For calculating the mean cover, the cover-abundance scores were transformed to a mean percentage score corresponding to the midpoint of each cover-abundance category: r = 0.05; + = 0.5; 1 = 2.5; 2 = 15.0; 3 = 37.5; 4 = 62.5; 5 = 87.5. Plant species were also assigned to plant growth form (PGF) categories (Supporting Information Appendix S4).

The environmental data from each plot include 107 variables, including site, soil, biomass, spectral data, NDVI and canopy structure variables. (see details in, Supporting Information Appendices S5.1 and S5.2, and the project data reports; Walker, Carlson, et al., 2011; Walker, Epstein, et al., 2008; Walker, Epstein, et al., 2009; Walker, Orekhov, et al., 2009).

Soils samples were collected from the uppermost mineral soil horizons at a point just outside the southwest corner of each vegetation plot. Larger soil pits were dug just outside the southwest corner of the 50 m × 50 m grid to fully describe vertical and horizontal variation in the soil profiles. The pits were described by Dr. Georgy Matyshak according the Russian approach and translated into descriptions corresponding to the US Soil Taxonomy approach (Soil Survey Staff, 1999) and are included with photographs in the data reports cited above.

2.2 | Climate

The Arctic bioclimate zonation patterns portrayed on the Circumpolar Arctic Vegetation Map (CAVM Team et al., 2003) are based primarily on summer temperature regimes and structure of the vegetation (Yurtsev, Tolmachev, & Rebristaya, 1978; Yurtsev, 1994a). We use the summer warmth index (SWI), which is the sum of monthly mean temperatures above 0°C, measured in °C month “thawing degree months”. The SWI is calculated from monthly mean

TABLE 1 Study locations, site numbers, site names, microsites, geological settings, parent material, and dominant vegetation at each study site

Location	Coordinates	Bioclimate subzone	Site	Geological setting[a], parent material	Microsite	Plot field numbers	Dominant vegetation
Krenkel	80°37′N, 58°03′E	A	KR-1, Loamy	Deluvial slope, perhaps old marine terrace at 30 m, sands		KR_RV_60–64	*Papaver dahlianum* spp. *polare*, *Stellaria edwardsii*, *Cetrariella delisei*, *Ditrichum flexicaule*, biological soil crust, cushion-forb, lichen, moss tundra
			Kr-2 Sandy	Recent marine terrace at 10 m, marine sands		KR_RV_65–69	*Papaver dahlianum* spp. *polare*, *Stellaria edwardsii*, *Cetrariella delisei*, biological soil crust, cushion-forb, lichen, moss tundra
Ostrov Belyy	73°19′N, 70°03′E	B	OB-1, loamy	Marine terrace II, alluvial-marine sediments, loamy facie of mixed sands and silts	OB-1a, Non-sorted circles	OB_RV_49a–53a	*Carex bigelowii*, *Calamagrostis holmii*, *Salix polaris*, *Hylocomium splendens*, graminoid, prostrate-dwarf-shrub, moss tundra
					OB-1b, Inter-circle areas	OB_RV_49b–53b	*Dryas integrifolia*, *Arctagrostis latifolia*, *Racomitrium lanuginosum*, *Ochrolechia frigida*, prostrate-dwarf-shrub, crustose-lichen barren
			OB-2, Sandy	Marine terrace I, alluvial-marine sediments, sands	OB-2a, Small non-sorted-polygon centres	OB_RV_54a–58a	*Gymnomitrion corallioides*-*Salix nummularia*-*Luzula confusa*-*Ochrolechia frigida*, liverwort, prostrate-dwarf-shrub, graminoid, lichen tundra
					OB-2b, Polygon cracks	OB_RV_53b–58b	*Racomitrium lanuginosum*, *Salix nummularia*, moss, prostrate-dwarf-shrub tundra
Kharasavey	71°12′N, 66°56′E	C	KH-1, loamy	Marine terrace II, marine silts		KH_RV_40–44	*Carex bigelowii*, *Calamagrostis holmii*, *Salix polaris*, *Dicranum elongatum*, *Cladonia* spp., graminoid, prostrate-dwarf-shrub, moss tundra
			KH-2a, sandy	Marine terrace I, marine silts		KH_RV_45–46	*Carex bigelowii*, *Salix nummularia*, *Dicranum* sp., *Cladonia* spp., graminoid, prostrate-dwarf-shrub, moss, lichen tundra
			KH-2b, sandy	Marine terrace II, marine sands and silts		KH_RV_47–49	*Salix nummularia*, *Luzula confusa*, *Polytrichum strictum*, *Sphaerophorus globosus*, prostrate-dwarf-shrub, graminoid, moss, lichen tundra
Vaskiny Dachi	70°17′N, 68°54′E	D	VD-1, loamy	Coastal marine plain terrace IV,, mixed Alluvial sands and marine silts		VD_RV_25–29	*Carex bigelowii*, *Vaccinium vitis-idaea*, *Hylocomium splendens*, sedge, dwarf shrub, moss tundra
			VD-2, loamy	Fluvial marine terrace III, mixed alluvial sands and marine silts		VD_RV_30–34	*Betula nana*, *Calamagrostis holmii*, *Aulacomnium turgidum*, erect-dwarf-shrub, graminoid, moss tundra
			VD-3, sandy	Fluvial terrace II, alluvial and aeolian reworked sands		VD_RV_35–39	*Vaccinium vitis-idaea*, *Cladonia arbuscula*, *Racomitrium lanuginosum*, prostrate-dwarf-shrub, sedge, lichen, tundra
Laborovaya	67°42′N, 68°01′E	E	LA-1, loamy	Glacial terrace, glacial silt		LA_RV_15–19	*Carex bigelowii*, *Betula nana*, *Aulacomnium palustre*, sedge, erect-dwarf-shrub, moss tundra

(*Continues*)

TABLE 1 (Continued)

Location	Coordinates	Bioclimate subzone	Site	Geological setting[a], parent material	Microsite	Plot field numbers	Dominant vegetation
			LA-2, sandy	Recent (<10 kya) alluvial terrace of stream, alluvial sand		LA_RV_20–21	*Betula nana*, *Vaccinium vitis-idaea*, *Sphaerophorus globosus*, *Polytrichum strictum*, prostrate-dwarf-shrub, lichen tundra
Nadym	65°19′N, 72°53′E	Forest–tundra transition	ND-1, loamy, forest	Fluvial terrace II, alluvial loamy sands		ND_RV_01–05	*Pinus sylvestris*, *Betula tortuosa*, *Rhododendron tomentosum*, *Cladonia stellaris*, erect-dwarf-shrub, lichen woodland
			ND-2, sandy, tundra	Fluvial terrace III, alluvial sands	ND-2a, Hummocks	ND_RV_06–08	*Rhododendron tomentosum*, *Betula nana*, *Cladonia stellaris*, erect-dwarf-shrub, lichen tundra
					ND-2b, Interhummocks	ND_RV_09–11	*Cladonia stellaris*, *Carex glomerata*, lichen tundra

[a]Marine and alluvial terrace numbers (see Supporting Information Appendix S1), approximate elevations above mean sea level on the Yamal Peninsula, approximate ages: Marine terrace I, 7–12 m a.s.l., Sartansky-age (Last Glacial Maximum, Late Wiechselian), ≈10–25 ka; Marine terrace II, 10–25 m a.s.l., Karginsky-Zyransky-age (Middle Weichselian), ≈25–75 ka; Marine terrace III, 26–40 m a.s.l., Ermanovsky-age (Early Weichselian), ≈75–117 ka; Marine terrace IV, 40–45 m a.s.l., Kazantsevskaya-age (Eemian interglacial), ≈117–130 ka; Marine terrace V, 45–58 m a.s.l., Salekhardskaya age (Saalian), ≈130–200 ka.

temperature data and is very strongly correlated with thawing degree days, which require daily mean temperature to calculate. SWI is equivalent to the warmth index, *a*, used by Steve Young for the vascular plant flora of St. Lawrence Island, Alaska (Young, 1971). Four of the six EAT locations have long-term climate station data; for these locations, we calculated the SWI for air temperatures (SWI_a) at the standard 2 m height of weather station observations. To obtain consistent summer temperature data for all study locations over the same length of record, we used data from the thermal infrared channels of satellite-based Advanced Very High Resolution Radiometers (AVHRR, years 1982–2003; Comiso, 2003, 2006) to calculate SWI_g, the ground surface summer warmth index (SWI_g) within 12.5-km pixels containing the study locations (Bhatt et al., 2010). Consistent data for other climate factors, such as precipitation and wind, were not available across all study locations.

2.3 | Vegetation analysis

2.3.1 | Cluster analysis

We used a hierarchical dendrogram approach, available in PC-ORD to group the plots into clusters based on the similarity of their species compositions (MjM Software, Gleneden Beach, OR, US) via the JUICE 7.0 software (Tichý, 2002). The most meaningful separation of the 76 plots was achieved with the flexible beta group linkage method (β = −0.25) with the Sørensen distance measure and square root data transformation. We included species-level taxonomic determinations in the analyses, and we excluded taxa that were identified only to the genus level. To determine the optimal number of clusters providing the highest 'separation power' for the data set, we used the Crispness of Classification approach (Botta-Dukát, Chytrý, & Hájková, 2005) available through the Optimclass function in JUICE (Tichý, 2002). A synoptic table was prepared using the combined synoptic table function in JUICE. Taxa with high fidelity (modified phi coefficients ≥ 0.5) were interpreted as diagnostic for the group; taxa with very high fidelity (modified phi coefficients ≥ 0.8) were interpreted as highly diagnostic.

2.3.2 | Analysis of vegetation and environmental variables

We compared the trends of plant growth form (PGF) cover along the bioclimate gradient (SWI_g) for each layer of the plant canopy (tree and shrub layer, herb layer and cryptogam layer); and the species richness within groups of dominant PGFs (deciduous shrubs, evergreen shrubs, graminoids, forbs, mosses, lichens). We also examined trends of soil properties along the bioclimate gradient.

2.3.3 | Ordination

We explored several ordination methods available in the R program (R Foundation for Statistical Computing, Vienna, AT) through the JUICE vegetation analysis package (Tichý, 2002). Detrended

Correspondence Analysis (DCA; Hill & Gauch, 1980) provided the clearest, most easily interpreted separation of plots along complex environmental gradients. Plot and species similarities were calculated using the Sørenson similarity index. Rare species were downweighted and the axes scaled according to the program defaults. The four main DCA axes 1, 2, 3 and 4 were correlated with continuous and ordinal environmental variables in each plot using species–environment correlations in the program CONOCO via JUICE. Only variables with $p \leq 0.002$ determined by global permutation test with forward selection (number of permutations: 499) are shown in the biplot diagrams.

3 | RESULTS

3.1 | Descriptions of the EAT locations and study sites

An overview of the study sites (Table 1) includes the study locations, coordinates, bioclimate subzones, study site numbers, geological setting, parent material, field plot numbers and dominant vegetation. Descriptions and photos of the environment and vegetation of each study location and study site are in Supporting Information Appendix S3. The species and environmental data from the 79 sample plots are in Supporting Information Appendices S4 and S5.

Mean July temperatures range from 1°C at Krenkel to 15.8°C at Nadym. Mean annual precipitation ranges from 258 mm at Ostrov Belyy to 479 mm at Nadym (Table 2). The SWI_g values at the EAT study locations are generally within one *SD* of the circumpolar SWI_g means of bioclimate subzones B to E (Table 2, columns 6 and 7), which indicates that these locations are representative of the mean zonal summer temperature conditions. The exception is Krenkel (SWI_g = 2°C month), which is much colder than the mean SWI_g for subzone A (8.2 ± 3.4°C month). The 12.5 km pixels of the satellite-derived SWI_g are subject to subpixel effects arising from the contrasting temperature regimes of different surfaces, especially near glaciers and coastlines (Smith, Reynolds, Peterson, & Lawrimore, 2008); however, the satellite-derived SWI_g values are within 1°C month of the station SWI_a values at all EAT study locations where station data are available, including the three coastal locations, (Table 2, columns 5 and 3).

Clay, silt and sand percentages for loamy and sandy sites are shown using the US Department of Agriculture soil texture triangle (Figure 2a). Loamy sites had 19%–61% sand and 31%–62% silt. Sandy sites generally had >80% sand, and <20% silt. Clay percentages were low (<25%) at all sites. On the loamy sites, silt and clay percentage were somewhat higher in the central part of the summer temperature gradient. Sand percentages were higher at both ends of the gradient (Figure 2b).

3.2 | Classification and syntaxonomic interpretation

The cluster analysis dendrogram shows the progressive linkage of plots according to their floristic similarity (Figure 3). Clusters with

TABLE 2 Temperature and precipitation along the Eurasia Arctic Transect. Mean (1961–1990) July temperature and precipitation data (columns 3 and 4) are from the nearest relevant climate stations. Summer Warmth Index (SWI) is the sum of the monthly mean temperatures above freezing. The mean atmospheric SWI (SWI_a) (column 5) is calculated from the mean (1961–1990) station data, where available. Ground Summer Warmth Indices (SWIg) (column 6) are calculated from AVHRR thermal bands for the 12.5-km pixels containing the EAT study locations. Value for SWI_g in the circumpolar Arctic subzones (column 7) are calculated using all circumpolar pixels within each subzone (Raynolds et al., 2008)

Bioclimate subzone	EAT study location	Mean July Temp. (1961–1990, °C)[a]	Mean annual precipitation (1961–1990, mm)[a]	Mean SWI_a at local climate station (1961–1990, °C month)[a]	Mean SWI_g for 12.5-km pixel containing the location (°C month)	Mean SWI_g for Circumpolar Arctic subzones (Mean ± *SD* °C month)
A	Krenkel	1	282	1.1	2.0	8.2 ± 3.4
B	Ostrov Belyy	5.6	258	11	11.5	12.6 ± 5.8
C	Kharasavey	7.2*	310*	18.6*	18.5	19.8 ± 5.1
D	Vaskiny Dachi	ND	ND	ND	29.6	27.0 ± 4.9
E	Laborovaya	ND	ND	ND	36.6	33.2 ± 4.4
FT-transition	Nadym	15.8	479	43	41.3	ND

[a]Leibman et al. (2012). *Data from Mare Sale, closest coastal station to Kharasavey, 100 km south.

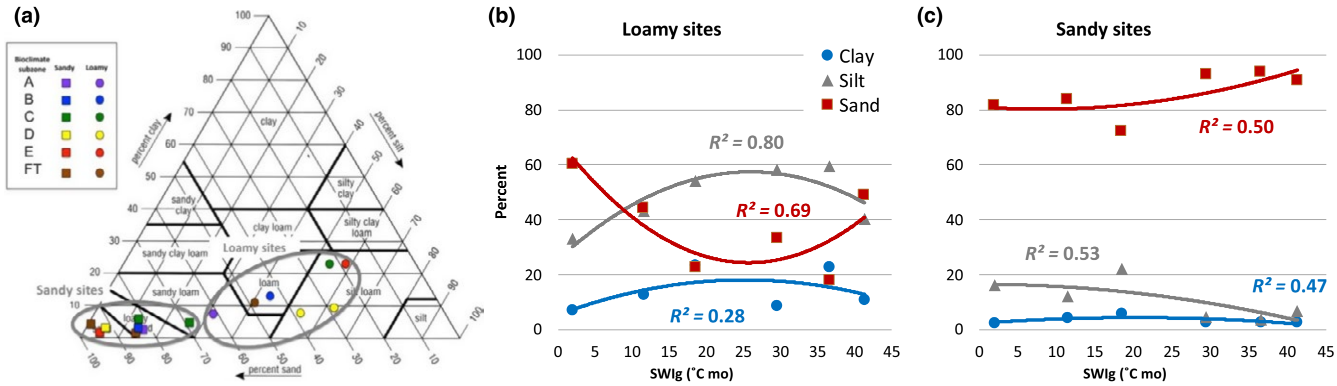

FIGURE 2 Mean soil textures for EAT loamy sites and sandy sites. (a) Mean soil texture classes for each site plotted on a USDA soil texture triangular (percentage sand, silt, clay) with 12 size classes defined by the US Department of Agriculture (Soil Survey Staff, 1999). Each point represents the mean of five plots except for the FT-sandy (brown squares), which portray mean values for hummocks (loamy sand) and inter-hummock (sand) plots. (b) Sand, silt and clay percentages at loamy sites vs. summer warmth index (SWI_g). (c) Sand, silt and clay percentages at sandy sites vs. summer warmth index (SWI_g). Best-fit regression equations are in Supplemental Information Appendix 9

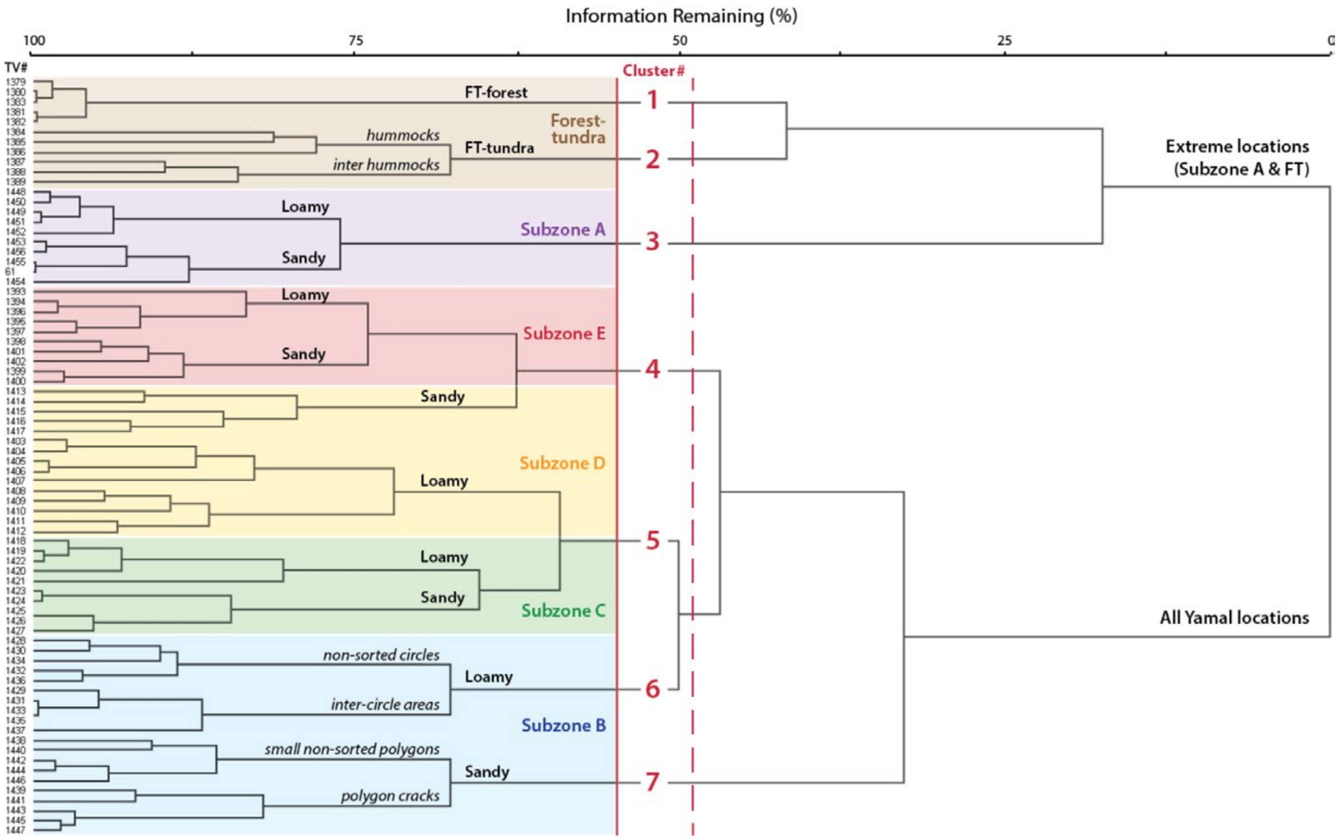

FIGURE 3 Cluster analysis of EAT plots. The plot is based on similarity of species composition within the 76 plots using Sørensen's coefficient of distance measure and square root data transformation. The numbers on the left side of the diagram are consecutive plot numbers assigned in the Turboveg program. Corresponding plot field numbers are in the Supporting Information Appendix S3. All species (vascular plants, bryophytes and lichens) were included. Plots linked toward the left side of the diagram have high species similarity; linkages toward the right side of the diagram have low levels of similarity. The flexible-β group linkage method (β = −0.25) was used to hierarchically link the plots. The vertical red dashed line shows the second optimal level of clustering based the Crispness of Classification approach (Botta-Dukát et al., 2005) available through the Optimclass function in JUICE (Tichý, 2002), which resulted in the six optimal clusters (red numbers). The red line is where the line was adjusted to separate out cluster 6, which based on field observations was distinct from cluster 5. Background colours correspond to the bioclimate subzones (A to Forest–tundra). Also shown are loamy and sandy groups of plots (black Roman labels), and micro-topographic groups of plots in patterned ground complexes (italics)

higher levels of similarity are toward the left side of the diagram. Crispness of Classification identified two clusters with the highest level of separability (dissimilarity). One cluster contained all of the Yamal plots (subzones B, C, D and E) and the other contained all the plots of FJL (subzone A) and Nadym (FT transition). The next highest level of dissimilarity was achieved with six clusters, separated at the level of the red dashed line in Figure 3. At this level, clusters 5 and 6 in Figure 3 were joined, forming one large cluster containing most of the plots on the Yamal Peninsula, including the subzone D loamy plots, all subzone C plots and the subzone B loamy plots. Based on our knowledge of the rather unique floristic character of the loamy subzone B site, which has characteristics similar to the moist non-acidic tundra described from North America, Greenland and Russia, we shifted the breakpoint for cluster definition slightly to the left so that the subzone B loamy plots were recognized as a separate cluster, resulting in a final grouping with seven clusters.

A synoptic table (Table 3) shows the frequency of species with very high fidelity (modified phi ≥ 0.8) and high fidelity (0.8 > modified phi ≥ 0.5). The full synoptic table, including diagnostic and non-diagnostic taxa, is in Supporting Information Appendix S6. Lists of the diagnostic, frequent and dominant taxa in each cluster are in Supporting Information Appendix S7. A summary of the contents of the clusters and their alignment with described Br.-Bl. syntaxa (mostly classes) are as follows:

Cluster 1 contains the five forest plots at Nadym with five highly diagnostic taxa (phi ≥ 0.8; *Pinus sylvestris*, *Betula pubescens*, *Larix sibirica*, *Vaccinium myrtillus*, *Juniperus communis*) and six other diagnostic taxa (phi ≥ 0.5). This cluster aligns with Cl. *Vaccinio–Piceetea* and All. *Vaccinio uliginosi–Pinion sylvestris* Br.-Bl (Braun-Blanquet). in Br.-Bl. et al. 1939, which contains Holarctic coniferous and boreo-subarctic birch forests on oligotrophic and leached soils in the boreal zone (Mucina et al., 2016).

Cluster 2 contains the six tundra plots in the forest–tundra transition at Nadym with three highly diagnostic taxa (*Carex globularis*, *Andromeda polifolia*, *Rubus chamaemorus*) and one other diagnostic taxon (*Rhododendron tomentosum*) This cluster aligns with Cl. *Oxycocco–Sphagnetea* Br.-Bl. et Tx. ex Westhoff et al. 1946, which contains dwarf shrub, sedge and peat moss vegetation of the Holarctic ombrotrophic bogs and wet heaths on extremely acidic soils.

Cluster 3 contains all ten plots in subzone A at Krenkel. This is the most distinctive cluster with 13 highly diagnostic taxa (*Stellaria edwardsii*, *Papaver dahlianum*, *Phippsia algida*, *Cochlearia groenlandica*, *Lecidea ramulosa*, *Orthothecium chryseum*, *Cladonia pocillum*, *Cetraria delisei*) and 18 other diagnostic taxa. Many of these are diagnostic for the recently described "polar desert" Br.-Bl. class *Drabo corymbosae–Papaveretea dahlilani* (Daniëls, Elvebakk, Matveyeva, & Mucina, 2016), which contains cushion forb, lichen, moss tundra occurring in polar deserts of the Arctic zone of the Arctic Ocean archipelagos (Mucina et al., 2016).

Clusters 4, 5, 6 and 7 form a broad group of plots across the central part of the Yamal Peninsula with a general trend from relatively warm sites in cluster 4 (subzones E and D) to relatively cold sites in clusters 6 and 7 (subzone B). Although all four clusters have several diagnostic taxa (phi > 0.5), there are only three highly diagnostic taxa (phi ≥ 0.8) in the group. *Cluster 4* contains the ten subzone E plots at Laborovaya and the five sandy plots in subzone D at Vaskiny Dachi. It has one highly diagnostic taxon (*Flavocetraria nivalis*) and eight other diagnostic taxa. This cluster aligns weakly with Cl. *Oxycocco–Sphagnetea* Br.-Bl. et Tx. ex Westhoff et al. 1946, which contains dwarf-shrub, sedge and peat-moss vegetation of the Holarctic ombrotrophic bogs and wet heaths on extremely acidic soils (Mucina et al., 2016). *Cluster 5* contains the ten subzone D loamy plots and ten subzone C plots. It has eight diagnostic taxa (*Lophozia ventricosa*, *Alopecurus borealis*, *Salix reptans*, *Eriophorum angustifolium*, *Tephroseris atropurpurea*, *Peltigera canina*, *P. aphthosa*, *Lichenomphalia hudsoniana*) and no highly diagnostic taxa. This cluster weakly aligns with Cl. *Scheuchzerio palustris–Caricetea fuscae* Tx. 1937, which contains sedge, moss vegetation of fens, transitional mires and bog hollows in the temperate, boreal and Arctic zones (Mucina et al., 2016). *Cluster 6* contains the five loamy plots at Ostrov Belyy, each of which has two microhabitat subplots corresponding to non-sorted circles and inter-circle areas. It has one highly diagnostic taxon (*Blepharostoma trichophyllum*) and eight other diagnostic taxa (*Salix polaris*, *Tomentypnum nitens*, *Dryas octopetala*, *Poa arctica*, *Juncus biglumis Bryum cyclophyllum*, *Stellaria longipes*, *Sphenolobus minutus*). This cluster weakly aligns with Cl. *Carici rupestris-Kobresietea bellardii* Ohba 1974, which contains, circum-Arctic fell-field and dwarf-shrub graminoid tundra on base-rich substrates (Mucina et al., 2016). It has characteristics of plant communities occurring on moist non-acidic soils in Alaska [Ass. *Dryado integrifoliae–Caricetum bigelowii* (Walker, Walker, & Auerbach, 1994)], Greenland [*Eriophorum angustifolium–Rhododendron lapponicum* comm. (Lünterbusch & Daniels, 2004)] and the Taimyr Peninsula, Russia [*Carici arctisibiricae–Hylocomietum alaskana* (Matveyeva, 1994)]. *Cluster 7* contains the ten subzone B sandy plots at Belyy Ostrov. It has one highly diagnostic taxon (*Pogonatum dentatum*) and 12 other diagnostic taxa (*Oxyria digyna*, *Gymnomitrion corallioides*, *Luzula confusa*, *Salix nummularia*, *Lloydia serotina*, *Solorina crocea*, *Polytrichum piliferum*, *Pohlia crudoides*, *Gowardia nigricans*). This cluster very weakly aligns with Cl. *Saxifrago cernuae–Cochlearietea groenlandicae* Mucina et Daniëls 2016, which contains vegetation of open graminoid tundra disturbed by cryoturbation (Mucina et al., 2016).

3.3 | Soils, vegetation structure and species richness

Trends of key soil and key vegetation canopy factors (canopy layer height, litter, standing dead, LAI, NDVI, total phytomass) vs. SWI_g are in Supporting Information Appendix S8.

Soil properties that increase with higher SWI_g include percentage sand (on sandy sites), thickness of organic horizons, percentage soil carbon (on loamy sites) and active layer thickness (Supporting Information Appendix S8, Figure S8-1). Soil properties that tend to

TABLE 3 Synoptic table containing diagnostic taxa for statistical clusters of mesic tundra vegetation plots along the Eurasia Arctic Transect

Cluster no.		1	2	4	5	6	7	3
Subzone(s) (soil texture)		**FT(lom)**	**FT(snd)**	**E+D(snd)**	**D(lom)+C**	**B(lom)**	**B(snd)**	**A**
Number of plots		**5**	**6**	**15**	**20**	**10**	**10**	**10**
Diagnostic taxa for cluster 1	Growth form			.	.	.	.	.
Pinus sylvestris	tne	100	.	.	.	.	.	.
Betula pubescens	tbd	100	.	.	.	.	.	.
Larix sibirica	tnd	100	.	.	.	.	.	.
Vaccinium myrtillus	sdd	100	.	.	.	.	.	.
Juniperus communis	sle	80	.	.	.	.	.	.
Peltigera malacea	lfo	60	.	.	.	.	.	.
Pleurozium schreberi	bmp	100	17	47	5	.	.	.
Peltigera leucophlebia	lfo	100	.	13	50	20	.	.
Cladonia stellaris	lfr	100	83	20	.	.	.	.
Empetrum nigrum	sde	100	17	80	10	.	.	.
Vaccinium uliginosum	sdd	100	33	67	15	.	.	.
Diagnostic taxa for cluster 2								
Carex globularis	gs	.	100	.	.	.	.	.
Andromeda polifolia	sde	.	83	7	.	.	.	.
Rubus chamaemorus	sdd	.	83	7	.	.	.	.
Rhododendron tomentosum s. tomentosum	sle	100	100	73	.	.	.	.
Diagnostic taxa for cluster 4								
Flavocetraria nivalis	lfr	.	.	93	25	.	.	.
Salix phylicifolia	sld	.	.	67	10	.	.	.
Eriophorum vaginatum	gs	.	17	87	25	.	.	.
Pedicularis labradorica	fe	.	.	53	.	.	.	.
Asahinea chrysantha	lfr	.	.	40	.	.	.	.
Pertusaria dactylina	lc	.	.	47	.	.	10	.
Cladonia grayi	lfr	.	.	40	5	.	.	.
Schljakovia kunzeana	bl	.	.	33	.	.	.	.
Luzula wahlenbergii	gr	.	.	33	.	.	.	.
Diagnostic taxon for clusters 5 & 6								
Arctagrostis latifolia	gg	.	.	20	95	100	10	.
Diagnostic taxa for cluster 5								
Lophozia ventricosa	bl	.	.	40	80	.	.	.
Alopecurus borealis	gg	.	.	.	60	.	.	10
Salix reptans	sdd	.	.	13	55	.	.	.
Eriophorum angustifolium	gs	.	.	27	60	.	.	.
Tephroseris atropurpurea	fe	.	.	7	45	.	.	.
Peltigera canina	lfo	.	.	.	35	.	.	.
Peltigera aphthosa	lfo	.	.	.	40	10	.	.
Lichenomphalia hudsoniana	lfo	.	.	.	30	.	.	.

(Continues)

TABLE 3 (Continued)

Cluster no.		1	2	4	5	6	7	3
Subzone(s) (soil texture)		FT(lom)	FT(snd)	E+D(snd)	D(lom)+C	B(lom)	B(snd)	A
Number of plots		5	6	15	20	10	10	10
Diagnostic taxa for cluster 6								
Blepharostoma trichophyllum	bl	.	.	.	5	100	.	.
Salix polaris	sdd	.	.	.	50	100	.	.
Tomentypnum nitens	bmp	.	.	13	20	90	.	.
Dryas octopetala	sde	.	.	.	40	100	50	.
Poa arctica	gg	.	.	7	40	80	.	.
Juncus biglumis	gr	.	.	.	.	60	20	.
Bryum cyclophyllum	bma	.	.	.	.	40	.	.
Stellaria longipes	fe	.	.	.	25	60	.	.
Sphenolobus minutus	bl	.	.	73	80	100	20	.
Diagnostic taxa for cluster 7								
Pogonatum dentatum	bma	.	.	13	.	.	80	.
Oxyria digyna	fm	.	.	.	.	.	80	20
Gymnomitrion corallioides	bl	.	.	33	25	10	100	.
Luzula confusa	gr	.	.	.	60	10	100	.
Salix nummularia	sdd	.	.	27	50	.	100	.
Lloydia serotina	fe	.	.	.	.	.	50	.
Solorina crocea	lfo	.	.	.	.	.	50	.
Polytrichum piliferum	bma	.	.	7	.	10	50	.
Pohlia crudoides	bma	.	.	7	.	.	40	.
Gowardia nigricans	lfr	.	.	40	60	20	90	.
Diagnostic taxa for cluster 3								
Stellaria longipes taxon *edwardsii*	fe	.	.	.	.	.	.	100
Papaver dahlianum agg. (*P. cornwallisense*)	fm	.	.	.	.	.	.	100
Phippsia algida	gg	.	.	.	.	.	.	100
Cochlearia groenlandica	fm	.	.	.	.	.	.	100
Lecidea ramulosa	lc	.	.	.	.	.	.	100
Orthothecium chryseum	bmp	.	.	.	.	10	.	100
Cladonia pocillum	lfr	.	.	.	.	10	.	100
Cetrariella delisei	lfr	.	.	20	.	.	.	100
Cerastium nigrescens v. *laxum*	fm	.	.	.	.	.	.	80
Fulgensia bracteata	lc	.	.	.	.	.	.	80
Saxifraga cernua	fe	.	.	.	5	.	.	80
Draba subcapitata	fm	.	.	.	.	.	20	90
Cirriphyllum cirrosum	bmp	.	.	.	.	.	.	70
Cerastium regelii	fm	.	.	.	.	10	.	70
Encalypta alpina	bma	.	.	.	.	.	.	60
Solorina bispora	lfo	.	.	.	.	.	.	60
Bryum rutilans	bma	.	.	.	.	.	.	60

(*Continues*)

TABLE 3 (Continued)

Cluster no.		1	2	4	5	6	7	3
Subzone(s) (soil texture)		**FT(lom)**	**FT(snd)**	**E+D(snd)**	**D(lom)+C**	**B(lom)**	**B(snd)**	**A**
Number of plots		**5**	**6**	**15**	**20**	**10**	**10**	**10**
Saxifraga cespitosa	fm	.	.	.	.	.	.	60
Distichium capillaceum	bma	.	.	.	.	30	.	80
Cetraria aculeata	lfr	.	.	.	.	.	20	70
Pohlia cruda	bma	.	.	.	.	40	.	80
Gowardia arctica	lfr	.	.	.	.	.	.	50
Saxifraga oppositifolia	fm	.	.	.	.	.	.	50
Cladonia symphycarpia	lfr	.	.	.	.	.	.	50
Stereocaulon rivulorum	lfr	.	.	.	.	.	.	50
Polytrichastrum alpinum	bma	.	.	.	30	10	60	100
Bartramia ithyphylla	bma	.	.	.	.	.	10	50
Callialaria curvicaulis	bmp	.	.	.	.	.	.	40
Campylium stellatum v. *arcticum*	bmp	.	.	.	.	.	.	40
Ditrichum flexicaule	bma	.	.	.	5	40	.	70
Protopannaria pezizoides	lc	.	.	.	5	.	.	40

Notes. Values are frequency of the given plant taxon within the indicated cluster (see Figure 3). Fidelity of diagnostic species was calculated using the phi coefficient (Chytrý, Tichý, Holt, & Botta-Dukát, 2002) for individual clusters compared to the full suite of clusters. Diagnostic taxa are ordered according to descending fidelity (modified phi values). Taxa with very high fidelity (modified phi ≥ 0.8) have frequency values highlighted in dark grey; those with high fidelity (modified phi ≥ 0.5) are highlighted in light grey. The second column in the table contains the plant growth form for each species: bl, bryophyte, liverwort; bma, bryophyte, moss, acrocarpous; bmp, bryophyte, moss, pleurocarpous; bms, bryophyte, moss, sphagnoid; fe, forb, erect; fm, forb, mat, cushion or rosette; gs, graminoid, sedge; gg, graminoid, grass; gr, graminoid, rush; lc, lichen, crustose; lfo, lichen, foliose; lfr, lichen, fruticose; sle, shrub, low, evergreen; sld, shrub, low, deciduous; sde, shrub, dwarf, evergreen; sdd, shrub, dwarf, deciduous; tne, tree, needle-leaf, evergreen; tnd, tree, needle-leaf, deciduous; tbd, tree, broad-leaf, deciduous; vs, vascular plant, seedless. A dot (.) indicates no record of the indicated species in the indicated cluster.

decrease with SWI_g include soil pH, soil moisture and sodium concentration. Loamy sites have generally higher volumetric soil moisture, pH, cation exchange capacity (CEC), sodium, volumetric soil moisture, thicker organic soil horizons, more soil carbon and nitrogen and shallower thaw depth.

The height of the plant canopy, number of canopy layers, LAI, NDVI and total phytomass all generally increase with summer warmth (Figure 4 and Supporting Information Appendix S8, Figure S8.2). The only site with trees is the Nadym forest site (ND1), which has mean total tree cover of 26% (Figure 4a, left, brown portion of stacked bars), split between evergreen needle-leaf trees (*Pinus sylvestris* and *P. sibirica*), deciduous broad-leaf trees (*Betula pubescens*) and deciduous needle-leaf trees (*Larix sibirica*). (See Supporting Information Appendix S4 for the raw species cover estimates.) Low shrubs (40–200-cm tall) occur in subzones D and E and the forest–tundra (VD1, VD2, LA1, LA2, ND1 and ND2) and are most abundant on loamy soils (Figure 4a, left). Dwarf shrubs (<40-cm tall) occur in all subzones except subzone A, where woody plants are absent. Deciduous shrub cover (Figure 4a, centre) varies nearly linearly with SWI_g on loamy soils (R^2 = 0.91) and has a weak polynomial trend (R^2 = 0.38) on sandy soils. Evergreen shrub cover has an exponential trend on loamy soils (R^2 = 0.89) and sandy soils (R^2 = 0.61; Figure 4a, right). Deciduous and evergreen shrub height and LAI increase exponentially with SWI_g (Supporting Information Appendix S8, Figure S8-2).

Graminoids are dominant in the herbaceous layer in all subzones except subzone A, where forbs are most abundant (Figure 4b, left). Graminoid cover peaks at 40% in subzone D on loamy soils (Figure 4b centre). On sandy soils, graminoid cover peaks at approximately 20% in subzones C and E. Sedges dominate the graminoid cover in all

FIGURE 4 Plant-growth-form (PGF) cover and species richness trends along the summer-warmth (SWI_g) gradient. (a–c) PGF cover in the layers of the plant canopy (tree and shrub, herb and cryptogam). Left: Bar graphs of mean cover of plant growth forms at each location in loamy and sandy sites. Right: Trend lines of mean cover of major PGF groups (deciduous shrubs, evergreen shrubs, graminoids, forbs, bryophytes and lichens) vs. SWI_g. (d) Mean species richness vs. summer warmth (SWI_g). (a) Mean total species richness on loamy and sandy sites. (b) Mean species richness of major PFG groups on loamy sites. (c) Mean species richness of major PFG groups on sandy sites. Equations of the trend lines are in Supplementary Information, Appendix S9

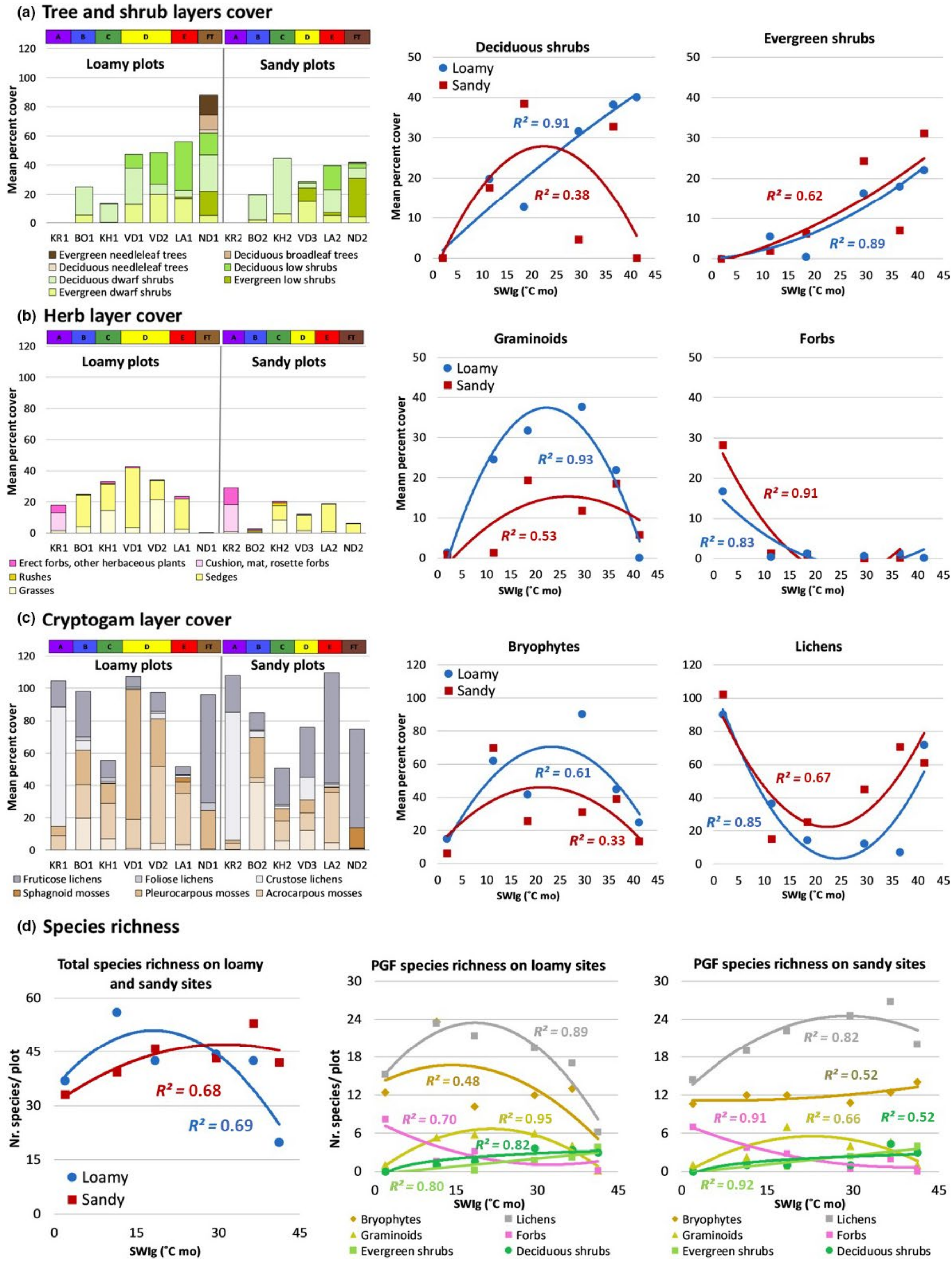
(a) Tree and shrub layers cover
Loamy plots
Sandy plots
Mean percent cover
KR1 BO1 KH1 VD1 VD2 LA1 ND1 KR2 BO2 KH2 VD3 LA2 ND2
Evergreen needleleaf trees
Deciduous broadleaf trees
Deciduous needleleaf trees
Deciduous low shrubs
Deciduous dwarf shrubs
Evergreen low shrubs
Evergreen dwarf shrubs
Deciduous shrubs
Loamy
Sandy
R^2 = 0.91
R^2 = 0.38
SWIg (°C mo)
Evergreen shrubs
R^2 = 0.62
R^2 = 0.89
(b) Herb layer cover
Erect forbs, other herbaceous plants
Cushion, mat, rosette forbs
Rushes
Sedges
Grasses
Graminoids
Meann percent cover
R^2 = 0.93
R^2 = 0.53
Forbs
R^2 = 0.91
R^2 = 0.83
(c) Cryptogam layer cover
Fruticose lichens
Foliose lichens
Crustose lichens
Sphagnoid mosses
Pleurocarpous mosses
Acrocarpous mosses
Bryophytes
R^2 = 0.61
R^2 = 0.33
Lichens
R^2 = 0.67
R^2 = 0.85
(d) Species richness
Total species richness on loamy and sandy sites
Nr. species/ plot
R^2 = 0.68
R^2 = 0.69
PGF species richness on loamy sites
R^2 = 0.89
R^2 = 0.48
R^2 = 0.70
R^2 = 0.95
R^2 = 0.82
R^2 = 0.80
PGF species richness on sandy sites
R^2 = 0.82
R^2 = 0.52
R^2 = 0.91
R^2 = 0.66
R^2 = 0.52
R^2 = 0.92
Bryophytes
Lichens
Graminoids
Forbs
Evergreen shrubs
Deciduous shrubs

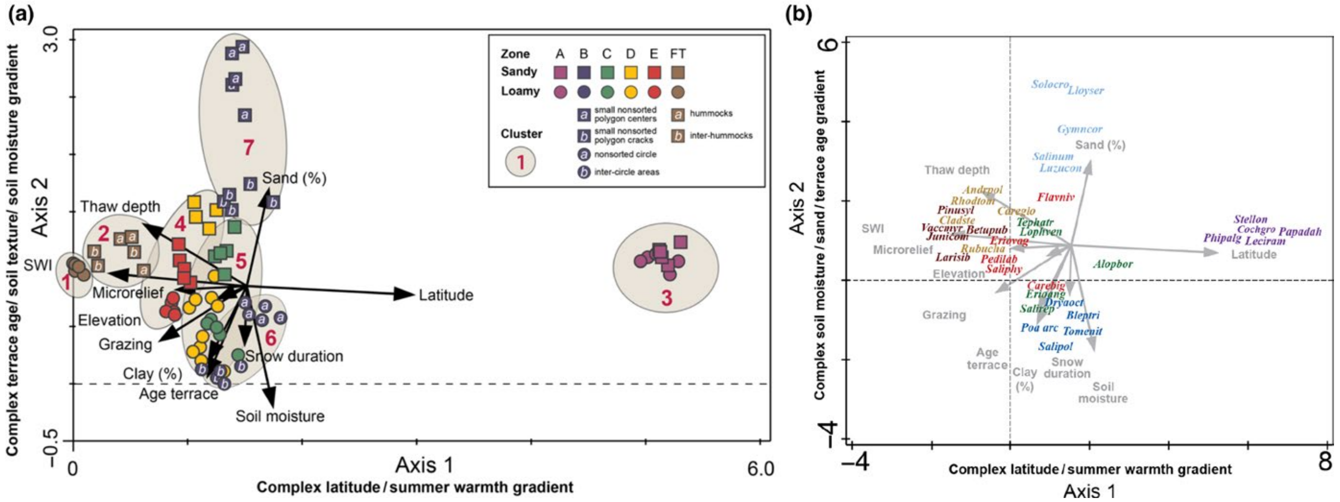

FIGURE 5 DCA ordination of EAT plots. (a) Plot ordination with environmental joint plot. Units along the axes are *SD* units, an indicator of the amount of species turnover in the data set. Four *SD* units are considered to represent approximately one complete species turnover. Plot symbols are colour-coded according to bioclimate subzones; shapes of symbols correspond to soil texture. Small letters (a, b) are microhabitats corresponding to patterned ground features at the Nadym Site ND-2 (hummocks and inter-hummocks) and Ostrov Belyy Site OB-1 (non-sorted circles and inter-circle areas) and Site OB-2 (small non-sorted polygon centres and cracks). Red cluster numbers are according to clusters in Figure 3. Joint-plot arrows denote direction and strength of correlations with environmental variables with $p \le 0.05$. (b) Species ordination. Centres of distributions are shown for the top five diagnostic taxa in each cluster. The alphabetic taxon codes are abbreviations containing the first four letters of the genus and first three letters of species names. Colours of taxa labels correspond to dominant bioclimate subzones of the clusters for which the taxa are diagnostic (Dark brown, cluster 1, FT-Forest; light brown, cluster 2, FT-tundra; red, cluster 4, subzone E & subzone D, sandy; green, cluster 5, subzone D, loamy & subzone C; dark blue, cluster 6, subzone B, loamy; light blue, cluster 7, subzone B, sandy; purple, cluster 3, subzone A.

subzones except subzone A, where sedges are absent. Sedges have generally higher cover on loamy sites compared to sandy sites. Grass cover is highest (>14%) on loamy soils in subzones C and D. Forbs occur with low cover in all subzones except subzone A, where they are the dominant component of the vascular plant cover (Figure 4b, right).

Lichens peak at both ends of the gradient on both loamy and sandy sites (Figure 4c, left and right). Fruticose lichens have highest cover in subzone E and the forest–tundra transition, exceeding 60% cover on loamy and sandy sites in the forest–tundra transition (ND1 and ND2); whereas crustose lichens (including biological crusts) have highest cover in subzone A, exceeding 80% cover on loamy and sandy sites (KR1 and KR2). Pleurocarpous mosses (those with branching growth forms, often forming carpets) are more abundant on loamy soils; whereas acrocarpous mosses (unbranched, often smaller mosses) are more abundant on acidic soils. Bryophyte cover peaked in the central part of the SWI_g gradient.

The range in total species richness at seven of the 12 sites was 39–46 species/plot, with extremes of 19.8 species/plot at the FT forest loamy site and 56 species/plot at the subzone B loamy site (Supporting Information Appendix S10, Figure 4d, left). The low species richness at the FT forest site (ND-1) is explained by the low diversity of cryptogams (6.2 lichen species and three bryophyte species), despite the very high cover of fruticose reindeer lichens. The high species richness at the subzone B loamy site (BO-1) is partly due to the presence of patterned ground and two distinct microhabitats (non-sorted circle centres and inter-circle areas) within the 5 m × 5-m plots.

The mean species richness is high in the cryptogam layer (lichens plus bryophytes, grey and brown lines in Figure 4d, centre and right), ranging between 25–47 species/plot at all sites except ND-1, which has 9.2 species/plot. The average total species richness ranges much more narrowly between 7.8 and 13.8 in the herb and shrub layers (Figure 4d). The various PGFs reach peak mean richness at different points along the bioclimate and soil-texture gradients: lichens, 26.8 species/plot (subzone E, sandy); bryophytes, 23.6 species/plot (subzone B, loamy); forbs, 8.2 species/plot (subzone A, loamy); graminoids, 7.4 species/plot (subzone D, loamy); deciduous shrubs, 4.4 species/plot (subzone E, sandy); evergreen shrubs, 4 specie/plot (forest–tundra transition, sandy); and trees, 3.4 species/plot (forest–tundra transition, loamy).

3.4 | Ordination

The DCA plot ordination (Figure 5a) displays the 76 plots according to their respective bioclimate subzone, texture class and cluster. Axis 1 has a high positive linear correlation with latitude (0.96) and a high negative correlation with SWIg (−0.77) (Supplementary Information Appendix S11). Plots in subzone A (cluster 3) are geographically and floristically widely separated from plots in the rest of the clusters, which form a large megacluster toward the left side of the ordination. Within the megacluster, there is generally a clear separation of plots in each of the statistical clusters, with transition from the relatively warm FT sites (clusters 1 and 2) on the left side of the megacluster to relatively cold subzone B (clusters 6 and 7) on the right side. There is relatively high floristic similarity among most of the plots in this megacluster, particularly among clusters 4, 5 and 6, indicating a continuous floristic gradient along the main Yamal Peninsula, rather than distinct vegetation units in each bioclimate subzone. Axis 2 has a strong positive correlation with sand percentage (0.64) and a strong negative correlation with soil moisture and terrace age (−0.75 and 0.51, respectively) (Supplementary Information Appendix S11). All sandy sites (coloured squares) are in the upper part the ordination, and loamy sites (coloured circles) are in the lower part.

The species ordination (Figure 5b) displays the centroids of distribution of five taxa with the highest fidelity to each of the seven clusters (35 total taxa). As expected, the centres of distributions for the diagnostic taxa generally align with the areas of the clusters for which they are diagnostic.

4 | DISCUSSION AND CONCLUSIONS

4.1 | Mesic vegetation transitions along the EAT summer temperature gradient

A primary motivation for this study was to develop a baseline of ground-based vegetation information along the complete Arctic summer temperature gradient in the maritime Arctic portion of western Russia to support remote sensing interpretations. We sampled and analysed plant communities on homogeneous mesic sites with loamy and sandy soils along the summer temperature gradient of the EAT. Satellite-derived summer land-surface temperatures (Comiso, 2006; Raynolds, Comiso, Walker, & Verbyla, 2008) provided a consistent spatial record of mean summer ground-surface temperatures (SWI_g) across the full length of the EAT, including locations where station data were unavailable.

The EAT analysis focused on mesic tundra areas where climate is the primary factor controlling the character of the vegetation. Although we initially considered these mesic sites to be zonal habitats, it soon became clear that the tundra over nearly the entire Yamal Peninsula is strongly influenced by a long history of reindeer grazing. The only locations that were free of recent reindeer foraging were Krenkel and Nadym at the extreme northern and southern ends of the bioclimate gradient. Both of these sites had high cover of lichens, indicating that reindeer at the other sites have greatly reduced the lichen cover. Reindeer herds graze heavily on lichens particularly during the snow-covered months of winter and spring. The results of our study and others (Pajunen, 2009; Pajunen, Virtanen, & Roininen, 2008; Vowles, Lovehav, Molau, & Björk, 2017; Yu, Epstein, Walker, Frost, & Forbes, 2011) and comparison with results from a similar transect in North America where there are relatively low *Rangifer* densities (Walker, Epstein, et al., 2012) indicate that the reindeer have had a long-term major impact on the shrub, graminoid and moss layers on the Yamal (Forbes et al., 2009). Quantifying this effect is difficult because of lack of reindeer exclusion areas.

Vegetation units described here for the middle portion of the EAT bioclimate gradient display gradual floristic transitions between bioclimate subzones and are only weakly aligned with previously described Br.-Bl. classes. A formal association-level classification for the Yamal region should await a broader analysis that includes new data collected within the past few years. Data from both the EAT and NAAT transects and additional data from zonal sites elsewhere in the Arctic should be used to develop a unified Braun-Blanquet classification for zonal vegetation across the full Arctic bioclimate gradient using the habitat-based approach of Mucina et al., 2016; Walker et al., 2018). There is especially a need for a new Br.-Bl. class corresponding to zonal acidic tundra in the middle part of Arctic bioclimate gradient. Additional studies are needed to develop clear Br.-Bl. syntaxa to characterize the variation along other important habitats and environmental gradients across the Arctic, including representative toposequences, riparian chronosequences, snowbed gradients and major disturbance gradients.

The analyses of trends of PGF cover and species richness within canopy layers vs. mean SWI_g provided quantitative data across the bioclimate gradient that support the observations of other investigators including: (a) the occurrence of progressively more and taller layers in the plant canopy with warmer temperatures (Elmendorf et al., 2012; Matveyeva, 1998), (b) increases in vascular plant cover and diversity along the summer temperature gradient (Daniëls et al., 2013; Rannie, 1986; Young, 1971), and (c) exclusion of woody plants, sedges and *Sphagnum* peat from the northernmost subzone A (Yurtsev, 1994b). While cover and species richness of evergreen and deciduous shrubs generally increased with higher SWI_g, cover of lichens and forbs declined. Graminoid cover and species richness of lichen and bryophyte species richness showed parabolic trends with maximum values in the central part of the temperature gradient.

Much recent research regarding productivity patterns in the Arctic has focused on the increased abundance of shrubs associated with warming temperatures, which are thought to be a primary cause of the recent increases in NDVI observed in satellite data (Myers-Smith et al., 2011). Our study documented strong, mostly positive, exponential trends with SWI_g for deciduous and evergreen shrub cover, shrub layer height, herb layer height, litter cover, LAI, NDVI and above-ground phytomass. The study also documented the dominance of shrubs in the Low Arctic (subzones E and D), dwarf shrubs, graminoids and bryophytes in the Middle Arctic (subzones C and B), and forbs and crustose lichens in the extreme High Arctic.

4.2 | The role of soil texture

The floristic contrast between the loamy and sandy sites varies considerably between locations across the EAT, a result of much greater site-factor heterogeneity of the sandy sites. The Nadym and Ostrov Belyy locations illustrate rather extreme contrasts in ecosystem structure that can occur on loamy vs. sandy soils. At Nadym, the site on the sandy, relatively young surface at ND-1 is relatively well drained, has no permafrost and is forested; whereas the ND-2 site on older, more fine-grained soils is ice-rich, relatively poorly drained, and covered with hummocky tundra vegetation (Supporting Information Appendix S3, Figure S3-6). A host of site factors interact to affect the vegetation structure and composition at this site, including much thicker soil organic layers, thin active layers, relatively cold soils and very low CECs on the older loamy soils. A similar contrast occurred at Ostrov Belly (Supporting Information Appendix S3, Figure S3-2) and is illustrated in the numerical classification and DCA ordination, where the sandy and loamy plots are placed in separate clusters (Figure 3, clusters 6 and 7) and are widely separated along Axis 2 of the ordination (Figures 3 and 5). The sandy sites at Ostrov Belyy are much drier than the loamy sites at this location and have many other site factor differences that separate them.

The opposite situation occurs at Krenkel (subzone A; Supporting Information Appendix S3, Figure S3-1), where both study sites have similar site factors with high floristic similarity and are placed in a single tight cluster in the ordination (cluster 3 in Figures 3 and 5). Loamy and sandy sites at Laborovaya (subzone E; Supporting Information Appendix S3, Figure S3-5) also have high floristic similarity, but in this case, there is also relatively high similarity with the sandy sites at Vaskiny Dachi (Supporting Information Appendix S3, Figure S3-4), so all three sites (LA-1, LA-2, VD-2,) are placed in a single numerical cluster (cluster 4 in Figures 3 and 5), with several acidophilic, oligotrophic, hypoarctic diagnostic species.

Part of the explanation for much larger variation in the sandy sites is that during site selection, it was relatively easy to find large sites to sample vegetation on mesic silt loam to sandy loam soils, whereas the availability of mesic very sandy sites was more limited. The relatively young sandy sites are also more susceptible to disturbance by reindeer and strong winds, whereas the older loamy sites have tended to stabilize toward the regional zonal conditions.

4.3 | Special importance of subzone A

A major accomplishment of this study was the first detailed vegetation description from exceptionally cold, wet and windy Hayes Island. Our results documented the high floristic dissimilarity of Hayes Island to the rest of the EAT (Figure 5), the dominance of biological soil crusts in the cryptogam layer and the dominance of forbs among the vascular plants (Figure 4b). It revealed a vegetation composed mainly of biological soil crusts, where even the vascular plants in the herb layer have cryptogam-like cushion and mat growth forms, unlike any other site along the EAT. Sites not exposed to excessive wind erosion had unexpectedly high hand-held NDVI (0.44–0.48), most likely caused by the high cover of wet biological soil crusts, which covered 50%–85% of the soil surface and comprised 33%–86% of the total biomass (Walker, Epstein, et al., 2012; Walker, Frost, et al., 2012). Rich fruticose lichen communities occurred on the most favourable zonal sites on Hayes Island, a result of the absence of reindeer (Supporting Information Appendix S12).

Numerous other studies have also noted the unique vegetation in subzone A (Chernov & Matveyeva, 1997; Daniëls et al., 2016) and its extreme susceptibility to climate change (Walker, Raynolds, & Gould, 2008). It is interesting that the total species richness of the coldest, most northern zonal location (Krenkel, KR-1, 37 species) is higher than that of the warmest most southern zonal location (Nadym, ND-1, 20 species; Supporting Information Appendix S12). The relatively high species richness at Krenkel is due to the large number of cryptogam species (24–27.8 species). Other arctic researchers have also noted high plot-scale cryptogam species richness at cold temperatures (Bültmann, 2005; Lünterbusch & Daniëls, 2004; Matveyeva,1998; Timling et al., 2012). In studies of Arctic lichen floras from subzone E to subzone A, the number of vascular plant species declines by approximately 95%, whereas the number of lichen species declines by only approximately 15% (Dahlberg, Bültmann, & Meltofte, 2013). The same authors note that the relatively small decline in lichen species at higher latitudes is due mainly to reductions in the number of lichens that normally grow on woody plants, which are greatly reduced toward the north. Increased availability of light due to reduced competition from herbs and shrubs is a major cause of high moss and lichen richness at the more northern sites (Marshall & Baltzer, 2015; Walker et al., 2006). Further competition for light occurs within very dense cryptogam layers in the southern locations, where a few reindeer lichen species with erect fruticose lichen growth forms (e.g. *Cladonia stellaris*, *C. stygia*, *C. rangiferina*, *C. arbuscular* and *C. mitis*) densely cover the ground of lichen woodlands and out-compete other species.

4.4 | Implications for Arctic climate change and ecosystem studies

Ground-based documentation of existing patterns of vegetation is a critical element of space-based monitoring of changes to terrestrial ecosystems during a time of rapid climate and land-use change in the Arctic (Stow et al., 2004). The patterns of vegetation greenness (NDVI) change have not been spatially or temporally consistent across the Arctic, due in part to the constantly changing patterns of sea ice in the Arctic basin (Bhatt et al., 2013) and changes in the growing season and productivity patterns ((Park et al., 2016). Although difficult logistics limit the number of sampling locations and the quantity of data that can be collected in the vast landscapes of the Arctic, there were advantages of these constraints during our studies because they facilitated interdisciplinary teamwork at the selected sites, assuring a largely spatially coherent database of vegetation, soil, permafrost and remote-sensing information to aid remote sensing interpretations and vegetation change modelling along a full maritime Arctic climate gradient. The research sites are permanently marked and provide a baseline against which to measure future vegetation change. The data should prove useful for interpretations of change to a wide variety of ecosystem properties and functions, including shrub growth (Myers-Smith et al., 2011), permafrost regimes (Romanovsky et al., 2017), Arctic tree lines (Harsch, Hulme, McGlone, & Duncan, 2009), snow distribution (Brown et al., 2017), regional hydrology (Prowse et al., 2017), soil carbon fluxes (Christensen et al., 2017), biodiversity (Meltofte, 2013) and land-use changes (AMAP 2010; Nymand & Fondahl, 2014). As sea ice retreats, it will be important to continue monitoring the changes from space, and also to continue to obtain ground-based information to document the consequences for the land surface (Bhatt et al., 2014). This is especially important in subzone A, which should be considered an endangered bioclimate subzone (Walker, Raynolds, et al., 2008).

ACKNOWLEDGEMENTS

Funding was mainly from the U.S. National Aeronautics and Space Administration, Land-Cover Land-Use Change Program (NASA LCLUC grants NNG6GE00A, NNX09AK56J, NNX14AD90G) with additional support from the Russian Academy of Science, the U.S. National Science Foundation Arctic Science Engineering and Education for Sustainability (NSF ArcSEES Award No. 1263854), the Bureau of Ocean Energy Management (BOEM) and the Slovak Academy of Science award VEGA 2/0135/16. We especially thank Marina Leibman, who led the Russian investigations and organized the logistics for the EAT expeditions. She and numerous other members of the Earth Cryosphere Institute made this study possible.

ORCID

Donald A. Walker https://orcid.org/0000-0001-9581-7811
Jozef Šibík https://orcid.org/0000-0002-5949-862X

REFERENCES

Alexandrova, V. D. (1980). *The arctic and antarctic: Their division into geobotanical areas*. Cambridge, UK: Cambridge University Press.

AMAP. (2010). *Assessment 2007: Oil and gas activities in the Arctic – effects and potential effects*. (Vol. 1 & 2; pp. 423–277). Oslo, Norway: Arctic Monitoring and Assessment Programme (AMAP). Retrieved from https://www.amap.no/documents/doc/assessment-2007-oil-and-gas-activities-in-the-arctic-effects-andpotential-effects.-volume-2/100

Belland, R. (2012). Arctic moss database. Retrieved 20 May 2016, cited in Raynolds, M. K., Breen, A. L., Walker, D. A., Elven, R., Belland, R., Konstantinova, N., … Hennekens, S. (2013) The Pan-Arctic Species List (PASL). Arctic Vegetation Archive Workshop, Krakow, Poland, 14-16 April 2013, CAFF Proceedings Series Report No. 10 (pp. 92–95).

Bhatt, U. S., Walker, D. A., Raynolds, M. K., Bieniek, P. A., Epstein, H. E., Comiso, J. C., … Polyakov, I. (2013). Recent declines in warming and vegetation greening trends over pan-Arctic tundra. *Remote Sensing*, *5*, 4229–4254. https://doi.org/10.3390/rs5094229

Bhatt, U. S., Walker, D. A., Raynolds, M. K., Comiso, J. C., Epstein, H. E., Jia, G., … Webber, P. J. (2010). Circumpolar Arctic tundra vegetation change is linked to sea ice decline. *Earth Interactions*, *14*, 1–20. https://doi.org/10.1175/2010EI315.1

Bhatt, U. S., Walker, D. A., Walsh, J. E., Carmack, E. C., Frey, K. E., Meier, W. N., … Simpson, W. R. (2014). Implications of Arctic sea ice decline for the Earth system. *Annual Review of Environment and Resources*, *39*, 57–89. https://doi.org/10.1146/annurev-environ-122012-094357

Bliss, L. C. (1997). Arctic ecosystems of North America. In F. E. Wielgolaski (Ed.), *Polar and alpine tundra* (pp. 551–683). Amsterdam, The Netherlands: Springer.

Botta-Dukát, Z., Chytrý, M., & Hájková, P. (2005). Vegetation of lowland wet meadows along a climatic contenentality gradient in Central Europe. *Preslia*, *77*, 89–111.

Braun-Blanquet, J. (1928). *Pflanzensoziologie. Grundzüge der Vegetationskunde. Biologische Studienbücher*, 7th ed. Berlin, Germany: Springer.

Brown, R., Schuler, D. V., Bulygina, O., Derksen, C., Luojus, K., Mudryk, L., … Yang, D. (2017). Arctic terrestrial snow cover. In AMAP (Ed.), *Snow, water, ice and permafrost in the arctic (SWIPA) 2017* (pp. 25–64). Oslo, Norway: Arctic Monitoring and Assessment Programme (AMAP).

Bültmann, H. (2005). Syntaxonomy of arctic terricolous lichen vegetation, including a case study from Southeast Greenland. *Phytocoenologia*, *35*, 909–949.

CAVM Team, Gould, W. A., Bliss, L. C., Edlund, S. A., Raynolds, M. K., Zoltai, S. C., … Walker, D. A. (2003). Circumpolar Arctic Vegetation Map. *Conservation of Arctic Flora and Fauna Map (CAFF) Map No. 1*. Anchorage, AK: U.S. Fish and Wildlife Service.

Chernov, Y. I., & Matveyeva, N. V. (1997). Arctic ecosystems in Russia. In F. E. Wielgolaski (Ed.), *Polar and alpine tundra* (pp. 361–507). Amsterdam, The Netherlands: Springer.

Christensen, T. R., Rysgaard, S., Bendtsen, J., Else, B., Glud, R. N., van Huissteden, K., … Vonk, J. E. (2017). Arctic carbon cycling. In AMAP (Ed.), *Snow, water, ice and permafrost in the arctic (SWIPA) 2017* (pp. 203–218). Oslo, Norway: Arctic Monitoring and Assessment Programme (AMAP).

Chytrý, M., Tichý, L., Holt, J., & Botta-Dukát, J. (2002). Determination of diagnostic species with statistical fidelity measures. *Journal of Vegetation Science*, *13*, 79–90. https://doi.org/10.1111/j.1654-1103.2002.tb02025.x

Comiso, J. C. (2003). Warming trends in the Arctic from clear sky satellite observations. *Journal of Climate*, *16*, 3498–3510. https://doi.org/10.1175/1520-0442(2003)016<3498:WTITAF>2.0.CO;2

Comiso, J. C. (2006). Arctic warming signals from satellite observations. *Weather*, *61*, 70. https://doi.org/10.1256/wea.222.05

Dahlberg, A., & Bültmann, H. (2013). Fungi. In H. Meltofte (Ed.), *Arctic Biodiversity Assessment: Status and trends in Arctic biodiversity* (pp. 355–371). Akureyri: Conservation of Arctic Flora and Fauna.

Daniëls, F. J., Bültmann, H., Lünterbusch, C., & Wilhelm, M. (2000). Vegetation zones and biodiversity of the North-American Arctic. *Berichte Der Reinhold-Tüxen-Gesellschaft*, *12*, 131.

Daniëls, F. J. A., Elvebakk, A., Matveyeva, N. V., & Mucina, L. (2016). The Drabo corymbosae-Papaveretea dahliani – a new vegetation class of the High Arctic polar deserts. *Hacquetia*, *15*, 5–13. https://doi.org/10.2307/3236190

Daniëls, F. J. A., Gillespie, L. J., Poulin, M., Afonina, O. M., Alsos, I. G., Aronsson, M., … Westergaard, B. K. (2013). Plants. In *Arctic biodiversity assessment* (pp. 310–345). Akureyri, Iceland: Conservation of Arctic Flora and Fauna.

Edlund, S. (1990). Bioclimate zones in the Canadian Archipelago. In C. R. Harrington (Ed.), *Canada's missing dimension: Science and history in the Canadian Arctic Islands* (pp. 421–441). Ottawa, ON, Canada: Canadian Museum of Nature.

Elmendorf, S. C., Henry, G. H. R., Hollister, R. D., Björk, R. G., Boulanger-Lapointe, N., Cooper, E. J., … Wipf, S. (2012). Plot-scale evidence of tundra vegetation change and links to recent summer warming. *Nature Climate Change*, *2*, 457. https://doi.org/10.1038/nclimate1465

Elvebakk, A., Elven, R., & Razzhivin, V. Y. (1999). Delimitation, zonal and sectorial subdivision of the Arctic for the Panarctic Flora Project. In I. Nordal & V. Y. Razzhivin (Eds.), *The species concept in the high north - A panarctic flora initiative* (pp. 375–386). Oslo, Norway: The Norwegian Academy of Science and Letters.

Elven, R., Murray, D. F., Razzhivin, V. Y., & Yurtsev, B. A. (2011). *Annotated checklist of the panarctic flora (PAF): Vascular plants*. Oslo, Norway:

National Centre of Biosystematics, Natural History Museum, University of Oslo.

Forbes, B. C., Stammler, F., Kumpula, T., Meschtyb, N., Pajunen, A., & Kaarlejärvi, E. (2009). High resilience in the Yamal-Nenets social-ecological system, West Siberian Arctic, Russia. *Proceedings of the National Academy of Sciences of the United States of America*, *106*, 22041–22048. https://doi.org/10.1073/pnas.0908286106

Gonzalez, G., Gould, W. A., & Raynolds, M. K. (2000). *1999 Canadian transect for the circumpolar arctic vegetation map*. AGC data report (p. 89). Fairbanks, AK: University of Alaska Fairbanks.

Harsch, M. A., Hulme, P. E., McGlone, M. S., & Duncan, R. P. (2009). Are treelines advancing? A global meta-analysis of treeline response to climate warming. *Ecology Letters*, *12*, 1040–1049. https://doi.org/10.1111/j.1461-0248.2009.01355.x

Hill, M. O., & Gauch, H. G. (1980). Detrended correspondence analysis, an improved ordination technique. *Vegetatio*, *42*, 47–58. https://doi.org/10.1007/BF00048870

Konstantinova, N. A., & Bakalin, V. A. (2009). Checklist of liverworts (Marchantiophyta) of Russia. *Arctoa*, *18*, 1–64. https://doi.org/10.15298/arctoa.18.01

Kristinsson, H., Hansen, E. S., & Zhurbenko, M. P. (2010). *Panarctic Lichen Checklist*. CAFF Technical Report nr. 20. Akureyri, Iceland: Conservation of Arctic Flora and Fauna, (pp. 1–120).

Leibman, M. O., Khomutov, A. V., Orekhov, P. T., Khitun, O. V., Epstein, H., Frost, G., & Walker, D. A. (2012). Gradient of seasonal thaw depth along the Yamal transect. In V. P. Melnikov, D. D. Drozdov, & V. E. Romanovsky (Eds.), *Tenth International Conference on Permafrost* (pp. 237–242). Salekhard: Volume Translations of Russian Contributions.

Lünterbusch, C. H., & Daniels, F. J. A. (2004). Phytosociological aspects of *Dryas integrifolia* vegetation on moist-wet soil in Northwest Greenland. *Phytocoenologia*, *34*, 241–270. https://doi.org/10.1127/0340-269x/2004/0034-0241

Marshall, K. E., & Baltzer, J. L. (2015). Decreased competitive interactions drive a reverse species richness latitudinal gradient in subarctic forests. *Ecology*, *96*, 461–470. https://doi.org/10.1890/14-0717.1

Matveyeva, N. V. (1994). Floristic classification and ecology of tundra vegetation of the Taymyr Peninsula, northern Siberia. *Journal of Vegetation Science*, *5*, 813–828. https://doi.org/10.2307/3236196

Matveyeva, N. V. (1998). *Zonation of plant cover in the arctic (Vol. 21)*. St. Petersburg, Russia: Russian Academy of Science.

Meltofte, H. (Ed.). (2013). *Arctic biodiversity assessment: Status and trends in arctic biodiversity*. Akureyri, Iceland: Conservation of Arctic Flora and Fauna.

Mucina, L., Bültmann, H., Dierßen, K., Theurillat, J.-P., Raus, T., Čarni, A., … Tichý, L. (2016). Vegetation of Europe: Hierarchical floristic classification system of vascular plant, bryophyte, lichen, and algal communities. *Applied Vegetation Science*, *19*(Suppl. 1), 3–264. https://doi.org/doi:10.1111/avsc.12257

Myers-Smith, I. H., Forbes, B. C., Wilmking, M., Hallinger, M., Lantz, T., Blok, D., … Hik, D. S. (2011). Shrub expansion in tundra ecosystems: Dynamics, impacts, and research priorities. *Environmental Research Letters*, *6*, 1–15.

Nymand, J., & Fondahl, G. (Eds.) (2014). *Arctic human development report: regional processes and global linkages*. Copenhagen: Nordic Council of Ministers.

Pajunen, A. M. (2009). Environmental and biotic determinants of growth and height of arctic willow shrubs along a latitudinal gradient. *Arctic, Antarctic, and Alpine Research*, *41*, 478–485. https://doi.org/10.1657/1938-4246-41.4.478

Pajunen, A., Virtanen, R., & Roininen, H. (2008). The effects of reindeer grazing on the composition and species richness. *Polar Biology*, *31*, 1233–1244. https://doi.org/10.1007/s00300-008-0462-8

Park, T., Ganguly, S., Tømmervik, H., Euskirchen, E. S., Høgda, K.-A., Karlsen, S. R., … Myneni, R. B. (2016). Changes in growing season duration and productivity of northern vegetation inferred from long-term remote sensing data. *Environmental Research Letters*, *11*, 8. https://doi.org/10.1088/1748-9326/11/8/084001

Polunin, N. (1951). The real Arctic: Suggestions for its delimitation, subdivision and characterization. *Journal of Ecology*, *39*, 308. https://doi.org/10.2307/2257914

Prowse, T. D., Bring, A., Carmack, E. C., Holland, M. M., Instanes, A., Mård, J., … Wrona, F. J. (2017). Freshwater. In AMAP (Ed.), *Snow, water, ice and permafrost in the arctic (SWIPA) 2017* (pp. 169–202). Oslo, Norway: Arctic Monitoring and Assessment Programme (AMAP).

Rannie, W. F. (1986). Summer air temperature and number of vascular species in arctic Canada. *Arctic*, *39*, 133–137.

Raynolds, M. K., Breen, A. L., Walker, D. A., Elven, R., Belland, R., Konstantinova, N., … Hennekens, S. (2013). *The Pan-Arctic Species List (PASL). Arctic Vegetation Archive Workshop, Krakow, Poland, 14-16 April 2013, CAFF Proceedings Series Report Nr. 10*. (pp. 92–95).

Raynolds, M. K., Comiso, J. C., Walker, D. A., & Verbyla, D. (2008). Relationship between satellite-derived land surface temperatures, arctic vegetation types, and NDVI. *Remote Sensing of Environment*, *112*, 1894. https://doi.org/10.1016/j.rse.2007.09.008

Razzhivin, V. Y. (1999). Zonation of vegetation in the Russian Arctic. In I. Nordal & V. Y. Razzhivin (Eds.), *The species concept in the high north - A panarctic flora initiative* (Vol. I. Mat.-Naturv. Klasse Skrifter, pp. 113–130). Oslo, Norway: The Norwegian Academy of Science and Letters.

Romanovsky, V., Isaksen, K., Drozdov, D., Anisimov, O., Instanes, A., Leibman, M., … Walker, D. (2017). Changing permafrost and its impacts. In AMAP (Ed.), *Snow, water, ice and permafrost in the arctic SWIPA 2017* (pp. 66–102). Oslo, Norway: Arctic Monitoring and Assessment Programme (AMAP).

Sieg, B., Drees, B., & Daniëls, F. J. A. (2006). Vegetation and altitudinal zonation in continental West Greenland. *Meddelelser Om Grønland, Bioscience*, *57*, 1–93.

Smith, T. M., Reynolds, R. W., Peterson, T. C., & Lawrimore, J. (2008). Improvements to NOAA's Historical Merged Land-Ocean Surface Temperature Analysis (1880–2006). *Journal of Climate*, *21*, 2283–2296. https://doi.org/10.1175/2007JCLI2100.1

Soil Survey Staff (1999). *Soil taxonomy: A basic system of soil classification for making and Interpreting soil surveys*, Vol. *436*. Washington, DC: U.S. Government Printing Office.

Stow, D. A., Hope, A., McGuire, D., Verbyla, D., Gamon, J., Huemmrich, F., … Mynenir, R. (2004). Remote sensing of vegetation and land-cover change in arctic tundra ecosystems. *Remote Sensing of Environment*, *89*, 281–308. https://doi.org/10.1016/j.rse.2003.10.018

Tichý, L. (2002). JUICE, software for vegetation classification. *Journal of Vegetation Science*, *13*, 451–453. https://doi.org/10.1111/j.1654-1103.2002.tb02069.x

Timling, I., Dahlberg, A., Walker, D. A., Gardes, M., Charcosset, J. Y., Welker, J. M., & Taylor, D. L. (2012). Distribution and drivers of ectomycorrhizal fungal communities across the North American Arctic. *Ecosphere*, *3*, 1–25. https://doi.org/10.1890/ES12-00217.1

Tuhkanen, S. (1984). A circumboreal system of climatic-phytogeographical regions. *Acta Botanica Fennica*, *127*, 1.

Vowles, T., Lovehav, C., Molau, U., & Björk, R. G. (2017). Contrasting impacts of reindeer grazing in two tundra grasslands. *Applied Vegetation Science*, *12*, 034018. https://doi.org/10.1088/1748-9326/aa62af

Walker, D. A., Carlson, S., Frost, G. V., Matyshak, G. V., Leibman, M. E., Orekhov, P., … Barbour, E. M. (2011). *2010 Expedition to Krenkel Station, Hayes Island, Franz Josef Land Russia. AGC data report*. Fairbanks, AK: University of Alaska.

Walker, D. A., Daniëls, F. J. A., Matveyeva, N. V., Šibík, J., Walker, M. D., Breen, A. L., … Wirth, L. M. (2018). Circumpolar Arctic Vegetation Classification. *Phytocoenologia*, *48*, 181–201. https://doi.org/10.1127/phyto/2017/0192

Walker, D. A., Epstein, H. E., Leibman, M. E., Moskalenko, N. G., Kuss, H. P., Matyshak, G. V., … Barbour, E. M. (2008). *Data report of the 2007*

Yamal expedition to Nadym, Laborovaya, and Vaskiny Dachi, Yamal Peninsula region, Russia. AGC Data Report.
Walker, D. A., Epstein, H. E., Leibman, M. E., Moskalenko, N. G., Kuss, J. P., Matyshak, G. V., … Barbour, E. M. (2009). *Data Report of the 2007 and 2008 Yamal Expeditions: Nadym, Laborovaya, Vaskiny Dachi, and Kharasavey. AGC Data Report* (p. 133). Fairbanks, AK: University of Alaska.
Walker, D. A., Epstein, H. E., Raynolds, M. K., Kuss, P., Kopecky, M. A., Frost, G. V., … Tichý, L. (2012). Environment, vegetation and greenness (NDVI) along the North America and Eurasia Arctic transects. *Applied Vegetation Science*, *7*, 015504. https://doi.org/10.1088/1748-9326/7/1/015504
Walker, D. A., Frost, S., Timling, I., Raynolds, M. K., Matyshak, G., Frost, G. V., … Afonina, O. (2012). High cover, biomass, and NDVI of biological soil crusts on Hayes Island, Franz Josef Land, Russia. In K. M. Hinkel & V. P. Melnikov (Eds.), (Vol. 4, pp. 634–635). *Presented at the Tenth International Conference on Permafrost, extended abstracts*. Salekhard: Northern Publisher.
Walker, D. A., Kuss, P., Epstein, H. E., Kade, A. N., Vonlanthen, C. M., Raynolds, M. K., & Daniëls, F. J. A. (2011). Vegetation of zonal patterned-ground ecosystems along the North America Arctic bioclimate gradient. *Applied Vegetation Science*, *14*, 440–463. https://doi.org/10.1111/j.1654-109X.2011.01149.x
Walker, D. A., Orekhov, P., Frost, G. V., Matyshak, G., Epstein, H. E., Leibman, M. O., … Maier, H. A. (2009). *The 2009 Yamal Expedition to Ostrov Belyy and Kharp, Yamal Region, Russia. AGC Data Report* (p. 63). Fairbanks, AK: University of Alaska Fairbanks.
Walker, D. A., Raynolds, M. K., Daniëls, F. J. A., Einarsson, E., Elvebakk, A., Gould, W. A., … Yurtsev, B. A. (2005). The Circumpolar Arctic Vegetation Map. *Journal of Vegetation Science*, *16*, 282. https://doi.org/10.1658/1100-9233(2005) 016[0267:TCAVM]2.0.CO;2
Walker, D. A., Raynolds, M. K., & Gould, W. A. (2008). Fred Daniëls, subzone A, and the North American Arctic Transect. *Abhandlungen aus dem Westfälischen Museum für Naturkunde*, *70*, 387–400.
Walker, M. D., Wahren, C. H., Hollister, R. D., Henry, G. H. R., Ahlquist, L. E., Alatalo, J. M., … Wookey, P. A. (2006). Plant community responses to experimental warming across the tundra biome. *Proceedings of the National Academy of Sciences of the United States of America*, *103*, 1342–1346. https://doi.org/10.2307/30048374?ref=search-gateway:ac394e72cab959e78c49a3ea70dc25e6
Walker, M. D., Walker, D. A., & Auerbach, N. A. (1994). Plant communities of a tussock tundra landscape in the Brooks Range Foothills, Alaska. *Journal of Vegetation Science*, *5*, 866. https://doi.org/10.2307/3236198
Walter, H. (1954). Klimax und zonale Vegetation. *Angewandte Pflazensoziologie, Festschrift Aichinger*, *1*, 144–150.
Walter, H. (1973). *Vegetation of the earth and ecological systems of the geo-biosphere. (J. Wieser, Trans.)*, 4th ed. New York, NY: Springer.
Westhoff, V., & Van der Maarel, E. (1978). The Braun-Blanquet approach. In R. H. Whittaker (Ed.), *Classification of plant communities* (pp. 287–399). Den Haag, The Netherlands: Junk. https://doi.org/10.1007/978-94-009-9183-5
Young, S. B. (1971). The vascular flora of St. Lawrence Island with special reference to floristic zonation in the arctic regions. *Contributions from the Gray Herbarium*, *201*, 11–115.
Yu, Q., Epstein, H. E., Walker, D. A., Frost, G. V., & Forbes, B. C. (2011). Modeling dynamics of tundra plant communities on the Yamal Peninsula, Russia, in response to climate change and grazing pressure. *Applied Vegetation Science*, *6*, https://doi.org/10.1088/1748-9326/6/4/045505
Yurtsev, B. A. (1994a). Latitudinal (zonal) and longitudinal (sectoral) phytogeographic division of the circumpolar arctic in relation to the structure of the vegetation map legend (Vol. 96, pp. 77–83). Presented at the Circumpolar Arctic Vegetation Mapping Workshop, Komarov Botanical Institute, St. Petersburg, RU: USGS.
Yurtsev, B. A. (1994b). The floristic division of the Arctic. *Journal of Vegetation Science*, *5*, 765–776. https://doi.org/10.2307/3236191
Yurtsev, B. A., Tolmachev, A. I., & Rebristaya, O. V. (1978). The floristic delimitation and subdivision of the Arctic. *The Arctic Floristic Region* (pp. 9–104). Leningrad: Nauka.

SUPPORTING INFORMATION

Additional supporting information may be found online in the Supporting Information section at the end of the article.

Appendix S1. Geological setting of the Yamal Peninsula.
Appendix S2. Typical plot layout.
Appendix S3. Eurasia Arctic Transect location and site descriptions.
Appendix S4. Eurasia Arctic Transect species cover-abundance data.
Appendix S5. Eurasia Arctic Transect environmental data.
Appendix S6. Full synoptic table.
Appendix S7. Diagnostic, constant, and dominant taxa for EAT clusters.
Appendix S8. Trends of selected soil and vegetation properties vs. summer warmth index.
Appendix S9. Regression equations for trend lines of analysed variables.
Appendix S10. Number of species per plot along the Eurasia Arctic Transect.
Appendix S11. Correlations between four axes of the DCA ordination and environmental variables.
Appendix S12. Lichen-rich tundra of Hayes Island.

How to cite this article: Walker DA, Epstein HE, Šibík J, et al. Vegetation on mesic loamy and sandy soils along a 1700-km maritime Eurasia Arctic Transect. *Appl Veg Sci*. 2019;22:150–167. https://doi.org/10.1111/avsc.12401

Marine and alluvial terraces of the Yamal Peninsula in relation to soil texture

Marine and alluvial terraces of varying age occur at all the locations along the Eurasia Arctic Transect (EAT) (Fig. S1-1). These terraces were formed during the postglacial emergence of northern Eurasia and the Franz Josef Land archipelago (Dibner, 1965; Forman et al., 2004; Ingólfsson, Möller, & Lokrantz, 2008; Saks, 1953; Svendsen et al., 2004). Relevant to this study, the older terraces (terraces III to V) generally have finer-grained loamy soils, and the younger terraces have sandy soils, providing the opportunity to compare differences in vegetation with respect to soil texture along the full bioclimate gradient. The older terraces also often have high concentrations of massive ground ice, and are extensively eroded by thawing permafrost and landslides (Ukraintseva, 2008, 2010). We selected loamy sites on broad well-drained hilltops of older terraces (III and IV) and sandy sites on younger terraces (I and II). (See Table 1 of main paper).

References:

Dibner, V. D. (1965). The history of late Pleistocene and Holocene sedimentation in Franz Josef Land (in Russian). *Transactions of the Scientific Research Institute of the Geology of the Arctic*, *143*, 300–318.

Forman, S. L., Lubinski, D. J., Zeeberg, J. J., Snyder, J. A., Siegert, M. J., & Matishov, G. G. (2004). A review of postglacial emergence on Svalbard, Franz Josef Land and Novaya Zemlya, northern Eurasia.

Ingólfsson, Ó., Möller, P., & Lokrantz, H. (2008). Late Quaternary marine-based Kara Sea ice sheets: a review of terrestrial stratigraphic data highlighting their formation. *Polar Research*, *27*(2), 152–161. http://doi.org/10.3402/polar.v27i2.6173

Saks, V. N. (1953). Quaternary period in the Soviet Arctic (in Russian) (pp. 1–627). Leningrad: Vdtransizdat.

Svendsen, J. I., Alexanderson, H., Astakhov, V., Demidov, I., Dowdeswell, J. A., Funder, S., et al. (2004). Late Quaternary ice sheet history of northern Eurasia. *Quaternary Science Reviews*, *23*(11-13), 1229–1271. http://doi.org/10.1016/j.quascirev.2003.12.008

Ukraintseva, N. (2008). Vegetation response to landslide spreading and climate change in the West SiberianTundra. In *Ninth International Conference on Permafrost* (pp. 1793–1798). Fairbanks.

Ukraintseva, N. (2010). High willow shrubs in Yamal: reasons of their wide expansion and methods of biomass assessment. Presented at the Second Yamal Land-Cover Land-Use Change Workshop, Rovaniemi, Finland.

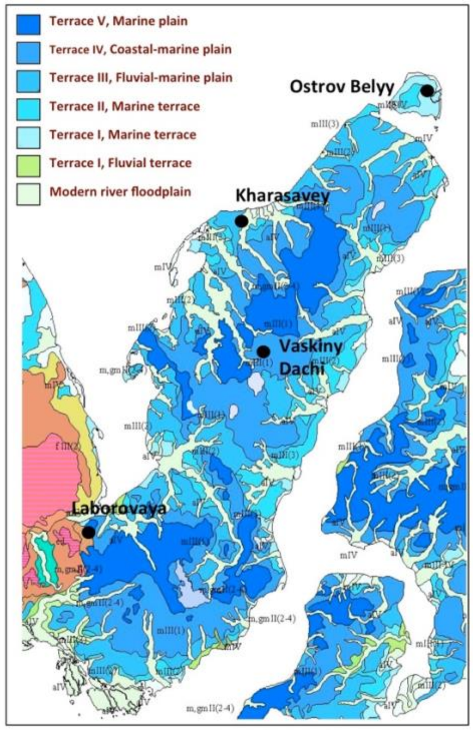

Figure S1-1. Quaternary-age terraces of the Yamal Peninsula. Terrace ages are still disputed; dates provided here are based mainly on Svendsen et al. (2004), with local glacial age names provided by the Earth Cryosphere Institute. Vegetation on starred (*) terraces was sampled during the EAT studies. *Terrace I, 7-12 m a.s.l., Sartansky-age (Last Glacial Maximum, Late Weichselian), ≈ 10-25 ka; *Terrace II, 10-25 m a.s.l., Karginsky-Zyransky-age (Middle Weichselian), ≈ 25-75 ka; *Terrace III, 26-40 m a.s.l., Ermanovsky-age (Early Weichselian), ≈ 75-117 ka; *Terrace IV, 40-45 m a.s.l., Kazantsevskaya-age (Eemian interglacial), ≈ 117-130 ka; Terrace V, 45-58 m a.s.l., Salekhardskaya age (Saalian), ≈130- 200 ka. The younger terraces (I, II) generally have sandy soils. Not shown are the marine terraces of Hayes Island (Dibner 1965). Sites on Hayes Island, FJL, are on sandy marine terraces at approximately 30 m a.s.l. and 10 m a.s.l. Graphic: Earth Cryosphere Institute.

Typical plot layout

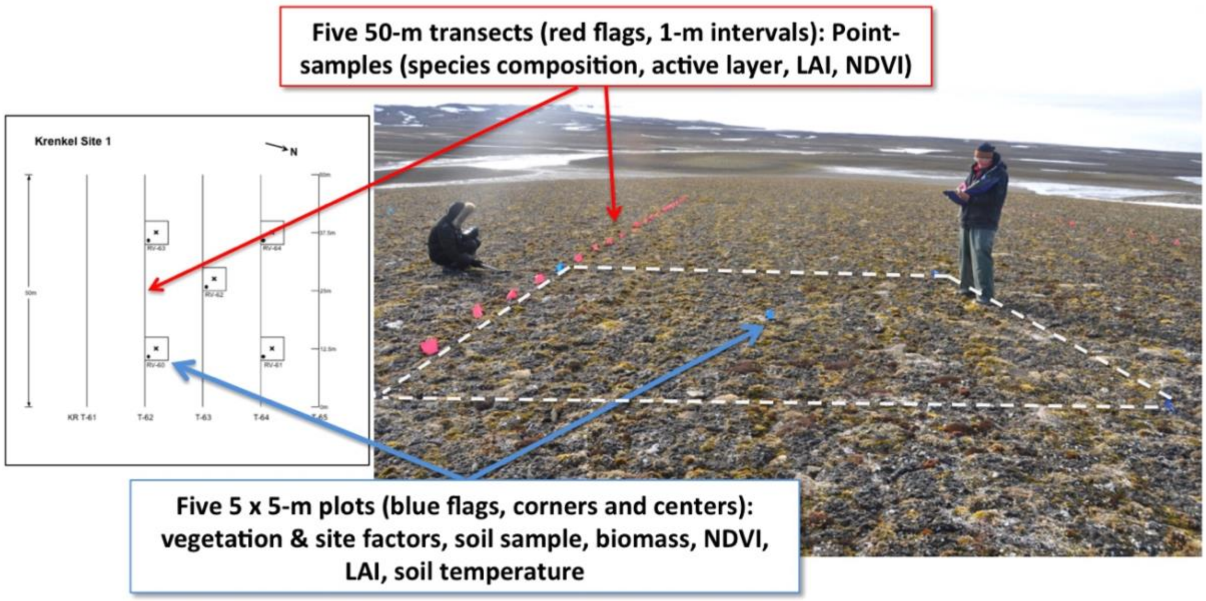

Figure S2-1. Typical plot layout. Five 5 x 5-m vegetation plots were located at 12.5, 25, and 37.5 m along the central three 50-m transects within 50 x 50-m areas of generally homogenous vegetation. In some cases, the position of a plot was adjusted to conform to areas of homogeneous vegetation. Additional data were collected along the five transects (red flags) at 0.5-m intervals. See text and D. A. Walker et al., 2008a for further details of data collection methods.

Eurasia Arctic Transect location and site descriptions

This appendix contains brief descriptions of research locations and study sites along the Eurasia Arctic Transect (EAT). Table 1 in the main paper provides a summary of locations, site numbers, site names, microsites, geological settings, marine and alluvial terraces, parent material, and dominant vegetation. Table 2 in the main paper provides the summary of climate information. More complete descriptions with additional photographs are in the project data reports (Walker et al., 2011; 2008; Walker, Epstein, et al., 2009a; Walker, Orekhov, et al., 2009b).

Krenkel

a.

b.

c.

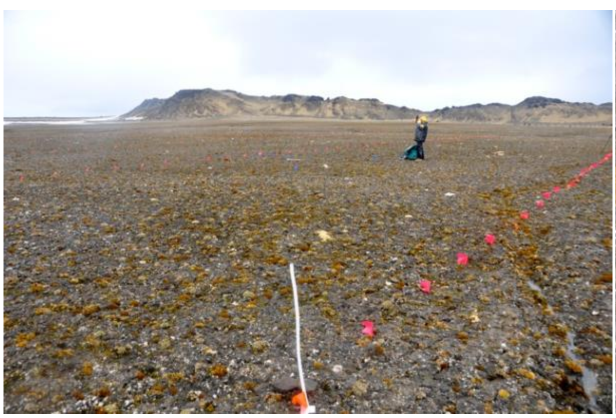

d.

Figure S3-1. Vegetation of the Krenkel (KR) EAT study location. a. KR, sandy-loam site, landscape view. **b.** Close-up of vegetation of KR-1. Dominant vascular plant species are *Papaver dahlianum* spp. *polare, Stellaria edwardsii, S. crassipes, Draba micropetala, Saxifraga cespitosa,* and *Phippsia algida*. Cushion forms of lichens and mosses include *Cetrariella delesii, C. islandica, Flavocetraria cucullata, Thamnolia subuliformis, Stereocaulon alpinum* and *S. rivulorum, Polytrichastrum alpinum, Orthothecium chryseon,* and *Bryum rutilans*. **c.** KR-2, sandy site, landscape view. **d.** Close up of the vegetation of KR-2. The dominant vascular plants are *Papaver dahlianum* spp. *polare, Stellaria edwardsii, S. crassipes, Saxifraga cernua, Phippsia algida* and *Cochlearia groendlandica.* Important cryptogamic species include the white lichen *Stereocaulon alpinum*. Note the small nonsorted polygons with plants growing preferentially in the cracks between polygons; 50-85% of the polygon surfaces are covered by gray biological soil crusts, which include *Anthelia juratzkana, Protopannaria pezizoides, Lecidea ramulosa, Baeomyces rufus*, *Lepraria gelida, Ochrolechia inaequatula*, *Ochrolechia frigida*, *Pertusaria* cf. *coriacea,* unidentified lichen prothalli, and algal crusts. Photos: D.A. Walker.

Hayes Island is a small 132-km^2 landmass in the central part of the Franz Jozef Land (FJL) archipelago. Unlike most islands in FJL, the majority of Hayes Island is ice free, with exception of the small (approximately 20 km^2) semi-circular-shaped Hydrogeographers Ice Cap on the northern coast of the island. Our studies were conducted near the Krenkel Hydrometeorological Station in the northeast corner of the island (80˚ 37’ N, 58˚ 03’ E).

The lithostratigraphy and geomorphology of the archipelago are more similar to those of Svalbard and Sverdrup basin in Canada than they are to the Yamal Peninsula. Troughs of rift origin separate the islands and are overlain by thick sedimentary sequences (Dibner, 1965). Basalt cliffs occur along the southern coast of Hayes Island, and numerous volcanic dikes cross the island to provide varied topography with rugged ridges and pinnacles. Most of the island is hilly and covered with sandy sedimentary deposits that are eroded by snow-melt streams. Mesozoic-age sandstones outcrops occur along stream channels, hills, and near Hydrographers Ice Cap, forming badland topography in some areas (Koryakin & Shipilov, 2009). Along the coast, unconsolidated marine deposits up to 10 m thick were formed as the island emerged following the last glacial maximum (Lubinski et al. 1999, Forman et al. 2004).

The maritime influence of the Barents Sea has a strong cooling effect on summer temperatures of the island. Cloudiness, summer fog and frequent storms are typical. High relative air humidity (80-92%) occurs all the year. The mean annual precipitation is 282 mm with the maximum precipitation occurring during October to March. The mean July temperature is only 1 ˚C, and the air summer warmth index (SWI_a) is a remarkably low 1.1 ˚C mo. The satellite-derived ground SWI_g is 1.86 ˚C mo. Strong northeasterly to southeasterly winds predominate in the winter, spring, and fall forming deep snow drifts that persist all summer in the stream networks. Hurricanes with the wind speeds up to 40 m/s are possible during this period. Extreme winds are comparatively rare in the summer.

Hayes Island has the most unique vegetation along the EAT. It is located in the Polar Desert geobotanical subregion (Alexandrova, 1980) and bioclimate subzone A of the Circumpolar Arctic Vegetation Map (CAVM Team 2003). No previous vegetation surveys are known from the island. Two sites were selected for the vegetation surveys.

KR-1, loamy site (Fig. S3-1a and b), is located on a gentle west-facing slope at an elevation of 30 m with relatively abundant plant cover. The surficial deposits are deluvium derived from the unconsolidated sandstone bedrock. Small non-sorted polygons, 10–15 cm in diameter, are common on most surfaces. These are formed by seasonal frost cracking. The cracks between the small polygons are protected habitats for small mosses, lichens and forbs (Fig. S3-1b). We did not separate the microhabitats associated with centers and cracks of these polygons, as we did on Ostrov Belyy, because of the small size of the polygons and difficulty in defining the boundaries of the communities.

KR-2, sandy site (Fig. S3-1c and d), is located on a flat sandy marine terrace at about 10-m elevation. The site has scattered glacially derived rocks. The surface has large flat-centered ice-wedge polygons 20–25 m in diameter, within these are small nonsorted polygons 10–20 cm in diameter. Differences between the two sites are rather small compared to the other EAT locations. KR-2 is more sparsely vegetated than KR-1 with about 7–15% cover of vascular plants. Cryptogamic crusts are more abundant than at KR-1, covering about 80–85% of the surface. The dominant vascular plants at both sites are *Papaver dahlianum* spp. *polare, Stellaria edwardsii, S. crassipes, Saxifraga cernua, Phippsia algida* and *Cochlearia groendlandica.* Cushion forms of the lichens *Cetrariella delesii, C. islandica, Flavocetraria cucullata, Thamnolia subuliformis, Stereocaulon alpinum and S. rivulorum* are common. Common bryophytes include *Polytrichastrum alpinum, Orthothecium chryseon, Bryum rutilans* and *Anthelia juratzkana.*

Ostrov Belyy (White Island)

a. b.


c. d.


Figure S3-2. Vegetation of the Ostrov Belyy (BO) EAT study location. a. BO-1, loamy site, landscape view from the southeast corner. The polar station is in the background. **b.** Vegetation and nonsorted circles within OB-1. Diameter of the circles is approximately 50 cm. The common plant species in the moist graminoid-dominated areas between the circles include *Carex bigelowii, Salix polaris, Calamagrostis holmii, Arctagrostis latifolia, Poa arctica, Hylocomium splendens, Aulacomnium turgidum, Dicranum spp., Ptilidium ciliare, Polytrichum strictum, Sphaerophorus globosus,* and *Cladonia arbuscula.* The centers of circles are more barren and drier; the dominant species are *Dryas integrifolia, Arctagrostis latifolia, Salix polaris, Racomitrium lanuginosum, Sphaerophorus globosus, Ochrolechia frigida, Bryocaulon divergens* and *Anthelia juratskana*). **c.** BO-2, sandy site, landscape view. **d.** Vegetation and small nonsorted polygons at OB-2. Diameter of the polygons is about 20-50 cm. The gray crust is composed primarily of the liverwort, *Gymnomitrion corallioides*. The moss in the polygon cracks is *Racomitrium lanuginosum*. Other common species include *Salix nummularia* and *Luzula confusa*. (Photos: D.A. Walker.)

Ostrov Belyy is just north of the Yamal Peninsula in the Kara Sea. The 15–30-km wide Malygin Strait separates the island from the peninsula, but the two have been connected during periods of lower sea level. The area of the island is approximately 2000 km^2. Fieldwork was carried out near the M.V. Popov Polar Meteorological Station in the northwest corner of the island (73°19′ N, 70°03′ E). The station has been occupied since 1933 and has been used as a base for a variety of purposes including meteorological and oceanographic observations, hydrocarbon exploration, military operations, and atmospheric studies using rockets. Permafrost thickness of the marine sediments of the modern coastal wetlands is 30 m on the average, varying from 2–10 meters at the coastline and 50–80 m inland. Permafrost thickness averages approximately 125 m on Terrace I, and approximately 240 m on Terrace II (Orekhov, Slagoda, & Popov, 2017; Trofimov, 1975).

We recorded 65 species vascular plant species in the vicinity of the Popov station. The only other records from the island were by F.R. Kielling, who recorded 17 species during the Vega Expedition of A.E. Nordensköld (1878–79), and Olga Rebristatya, who recorded 75 species of vascular plants in the southeast part of the island (Rebristaya 1995).

The main part of the ground observations at Ostrov Belyy were conducted at two study sites: BO-1, loamy site (Fig. S3-2a and b), consists of zonal tundra. (Note the mistaken reversal of the B and O in our plot numbers for Ostrov Belyy). Zonal tundra on loamy soils is rare on the island because of the island's general wetness and abundance of sandy substrates. Reindeer, although not absent, are much less abundant than they are on the mainland. Small non-sorted circles (0.3–1 m diameters) (also called "frost boils") (Washburn, 1980) were common at BO-1, where we sampled plant communities of two microhabitats within the 5 x 5-m plots: BO-1a occurred in association with the moist graminoid-dominated habitats between non-sorted circles and BO-1b occurred on the more barren and drier centers of the circles.

BO-2, sandy site (Fig. S3-2c and d), is located on a low well-drained bluff of a small stream about two km southeast of the Popov station. Areas with sandy soils occur along most stream bluffs and lake margins that are relatively well-drained. The surfaces of many of these well-drained sites appear gray because of the low cover of vascular plants and high cover of the crustose liverwort *Gymnomitrion corallioides*. Similar habitats have recently been described in a study of mires on Ostrov Belyy (Makarova, Ermilov, Yurtaev, & Mansurov, 2015). Small non-sorted polygons, 10–30 cm in diameter, are abundant on this dry site, so we sampled the two main microhabitats of these polygons: BO-2a occurred in association with the dry *Gymnomitrion*-dominated habitats on the small-polygon centers, and BO-2b occurred in the mossy cracks between the polygons.

Kharasavey

a. b.

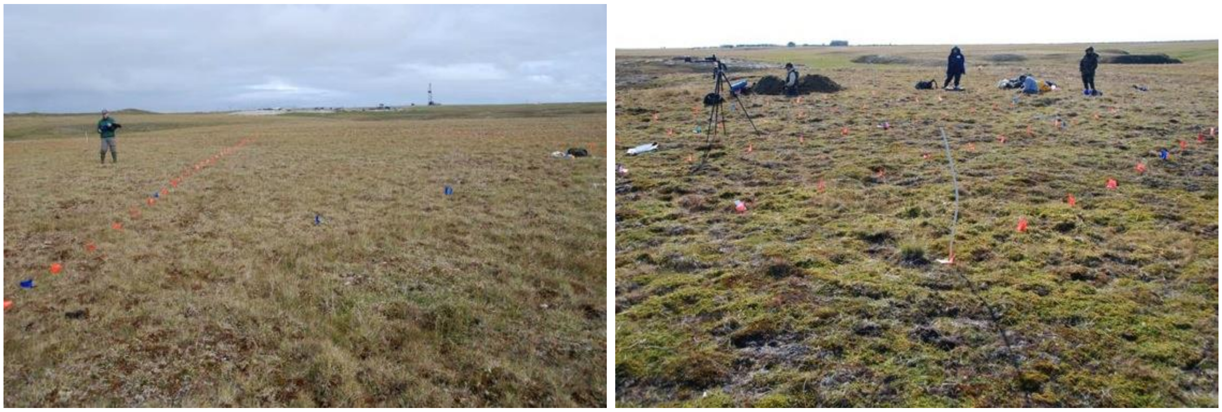

Figure S3-3. Vegetation of the Kharasavey (KH) study location. a. KH-1, loamy site. The vegetation is moist graminoid, prostrate dwarf-shrub, moss tundra, dominated by *Carex bigelowii, Calamagrostis holmii, Salix polaris, Dicranum elongatum* and *Cladonia* spp. b. KH-2b, sandy site. The vegetation is moist sedge, prostrate dwarf-shrub, moss tundra, dominated by *Carex bigelowii, Salix nummularia, Dicranum* sp., and *Cladonia* spp. (Photos: D.A. Walker.)

Kharasavey is located on the northwestern coast of the Yamal Peninsula (71°12' N, 66°56' E), approximately 60 km northwest of the Bovanenkovo gas field and 76 km northwest of Vaskiny Dachi. The area is part of a large complex of gas fields in west central Yamal. Pipelines and rail links are planned to Bovanenkovo. Kharasavey is also the endpoint of several reindeer-herd migration routes. Ongoing research at Bovanenkovo, Laborovaya and other locations on the Yamal is examining the social-ecological consequences of gas development and adaptations by the local Nenetsy people (Forbes, 2013; Kumpula, Forbes, Stammler, & Meschtyb, 2012). The flat to undulating local terrain is derived from sediments of marine terraces I and II (see Supplemental Information, Appendix S1). The terrace surfaces are relatively well drained and highly dissected by many small gullies and drainages. The drainages are continually expanding and growing due to erosion by cryogenic landslides of the underlying massive ground ice. Thermokarst features, including thaw lakes, drained thaw lakes, small thermokarst ponds, and ice-wedge polygons, are common in nearby peaty lowlands of the larger streams and rivers in the vicinity of Kharasavey.

There is no long-term climate record from Kharasavey. The nearest comparable coastal weather station is approximately 100 km south at Mare-Sale, where the mean annual air temperature (1961-1990) prior to the recent warming trend was -8.5 ˚C. The mean July temperature for the same period was 7.2 ˚C, and the air temperature summer warmth index (SWI_a) was 19.6 ˚C mo. The satellite-derived summer warmth index of the ground surface (SWI_g, 1982-2003) is 18.52 ˚C mo. The mean annual precipitation is 298 mm. The known local Kharasavey flora consists of 125 species of vascular plants (Rebristaya et al., 1995).

Four study sites were established at Kharasavey. KH-1, loamy site (Fig. S3-3a), is located on a homogeneous portion of terrace II with silt-loam soils. Common plants on the upland tundra areas include dwarf shrubs (e.g., *Salix polaris, S. lanata,* and *S. glauca*), graminoids (e.g, *Carex bigelowii, Calamagrostis holmii, Arctagrostis latifolia, Eriophorum angustifolium, Alopecurus alpinus, Poa arctica,* and *Luzula confusa*), forbs (e.g., *Saxifraga cernua, S. foliolosa,* and *Rumex* *arcticus)*, mosses (e.g., *Dicranum elongatum, Polytrichum strictum, Aulacomnium* spp., and *Hylocomium splendens*), and lichens (e.g., *Cladonia* spp., *Sphaerophorus globosus, Peltigera aphthosa, Thamnolia subuliformis,* and *Cetraria* spp.). Large areas with sandy soils were uncommon. Small dune-like remnant sandy features occur along some of the creeks, but no extensive sandy areas with sufficient flat homogeneous terrain for a 50 x 50-m grid could be located. Consequently, we selected two 10 x 10-m sandy areas along bluffs of two small streams and supplemented the vegetation data with another nearby 5 x 5-m plot. Kharasavey-2a (KH-2a, sandy site) is on a small bluff of terrace I adjacent to a creek with thin sands over much of the grid. KH-2b, sandy site (Fig. S3-3b), is on a sandy portion of terrace II, where the vegetation is dominated by *Carex bigelowii, Salix nummularia, Dicranum* spp., and *Cladonia* spp. Sites KH-2a and KH-2b had two plots each. The fifth sandy plot (KH-RV-49) was located on an adjacent sandy feature near site KH-2b.

Vaskiny Dachi

a. b.

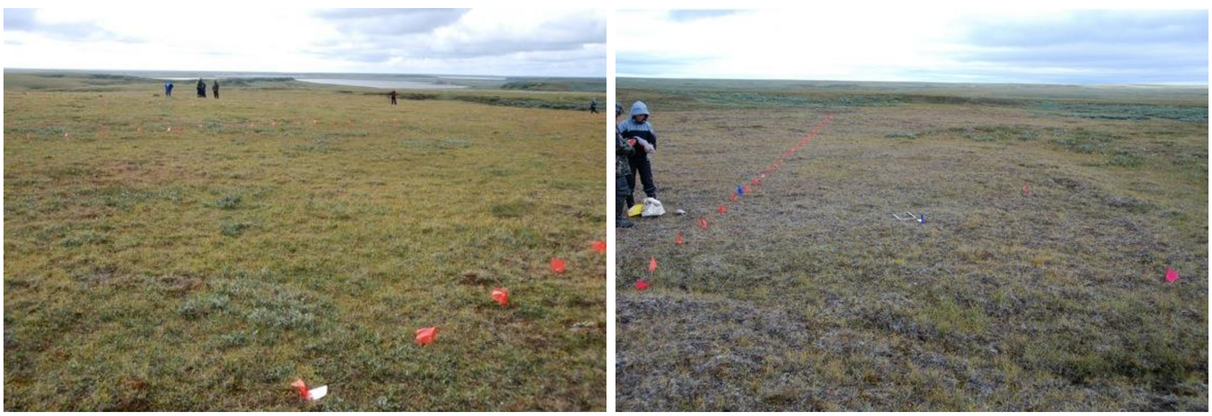

Figure S3-4. Vegetation of the Vaskiny Dachi EAT study location. a. VD-1, loamy site, on Terrace IV. The vegetation is heavily grazed sedge, dwarf-shrub, moss tundra dominated by *Carex bigelowii, Vaccinium vitis-idaea, Salix glauca, Hylocomium splendens,* and *Aulacomnium turgidum*. b. VD-3, sandy site, on Terrace II. The vegetation is a dry dwarf-shrub, lichen tundra dominated by *Carex bigelowii, Vaccinium vitis-idaea, Cladonia arbuscula, Sphaerophorus globosus, Racomitrium lanuginosum,* and *Polytrichum strictum*. (Photos: D.A. Walker.)

The location is approximately 1.4 km west of the Obskaya-Bovanenkovo railroad and 21 km east-southeast of the main airfield at the Bovanenkovo gas field, the largest gas field on the peninsula. The Vaskiny Dachi Research Station (VD) was established in 1988 to support Russian Academy of Science research associated with railroad construction and gas-field development on the Yamal Peninsula. Since 1993 it has been a major focus of research for the Circumpolar Active Layer Monitoring (CALM) project of Dr. Marina Leibman and colleagues from the Earth Cryosphere Institute (Leibman, Gubarkov, & Khomutov, 2012; Leibman, Khomutov, Gubarkov, Mullanurov, & Dvornikov, 2015).

Gentle hilly terrain is associated with a series of highly eroded marine terraces of various ages and floodplains of the widely meandering Se-Yakha and Mordy-Ykha rivers. Despite the long period of research, there is no climate station at Vaskiny Dachi because of difficulties associated with maintaining a site with the annual reindeer migrations through the area. The mean annual summer warmth index (SWI_g) derived from satellite data is 29.6 ˚C mo.

The Vaskiny Dachi area is within Arctic bioclimate subzone D. The landslides and associated botanical features of the central Yamal have received considerable attention (Ermokhina, 2009; Rebristaya & Khitun, 1998; Rebristaya, VV, Chernyadjeva, & Leibman, 1995). A striking aspect of the regional vegetation is the abundance of willow thickets (*Salix lanata, S. glauca*), which cover many hill slopes and valley bottoms in association with the landslides (Rebristaya & Khitun, 1998; Ukraintseva, 2008; Ukraintseva, Leibman, & Streletskaya, 2000; Ukraintseva, Streletskaya, Ermokhina, & Yermakov, 2003).

Three study sites were established at Vaskiny Dachi in stable areas that avoided the landslides. VD-1 (Fig. S3-4a) and VD-2, loamy sites, are on gentle hills associated with marine terraces III and IV (Kazantsevskaya and Ermanovsky-age). The soils are silt loams. The vegetation of VD-1 and VD-2 is heavily grazed sedge, dwarf-shrub-moss tundra, dominated by *Carex bigelowii, Vaccinium vitis-idaea, Salix glauca, Hylocomium splendens,* and *Aulacomnium turgidum* at VD-1, and by *Betula nana, Calamagrostis holmii,* and *Aulacomnium turgidum* at VD-2.

VD-3, sandy site (Fig. S3-4b), is on a more recent fluvial terrace (terrace II, Table 1), comprised of finely interbedded sandy, silty, loamy, and organic layers of several millimeters to several centimeters thick. Vegetation at this site is prostrate dwarf-shrub, sedge, lichen tundra dominated by *Vaccinium vitis-idaea, Cladonia arbuscula,* and *Racomitrium lanuginosum*.

Labororvaya

a. b.

Figure S3-5. Vegetation of the Laborovaya EAT study location. a. LA-1, loamy site. The vegetation is a moist dwarf-shrub, sedge, moss tundra dominated by *Betula nana, Vaccinium vitis-idaea, V. uliginosum, Carex bigelowii, Eriophorum vaginatum, Aulacomnium palustre, Hylocomium splendens, and Dicranum* spp. b. LA-2, sandy site. The vegetation is moist/dry dwarf-shrub, lichen tundra dominated by *Betula nana, Vaccinium vitis-idaea, V. uliginosum, Carex bigelowii, Cladonia arbuscula, Sphaerophorus globosus,* and *Polytrichum strictum*. (Photos: D.A. Walker.)

The Laborovaya location (67˚ 42’ N, 68˚ 01’ E) is in the foothills near the northern end of the Polar Urals, about 21 km northeast of the small settlement of Laborovaya at km 147 of the Obskaya-Paijuta railway/ road corridor. The local physiography consists of flat plains with thaw lakes to the east and north. Hills with glaciated sandstone bedrock outcrops occur to the west and south.

Surface sediments on the plains consist primarily of Pleistocene sands underlain by saline silts and clays, similar to the geological situation on the main part of the Yamal Peninsula. Laborovaya and all EAT locations north of here lie within the continuous permafrost zone. This is a long-term study location of Dr. Bruce Forbes and researchers at the Arctic Center, Rovaniemi, Finland (Forbes, 1997).

The nearest year-round meteorological station is at Salekhard, 150 km to the south, near the mouth of the Ob River, which is not comparable because Salekhard is in the forest and is warmer and calmer than the Laborovaya region, which is strongly affected by its proximity to the Polar Urals. The mean satellite-derived summer-warmth index (SWI_g) for Laborovaya is 36.6 ˚C mo.

Phytogeographically, the study site lies about 100 km north of the latitudinal treeline within the southern tundra subzone (Subzone E of the Circumpolar Arctic Vegetation Map). This area and all of the Yamal Peninsula is within the Yamal-Gydan West Siberian floristic subprovince, which is characterized by a low floristic richness due to gaps in the ranges of species with predominantly montane, east Siberian distributions and western (amphi-Atlantic) distributions (Yurtsev, 1994). The region's vegetation has been mapped and described at small scale according to the Russian approach to vegetation classification (Ilyina, Lapshina, Makhno, Meltzer, & Romanova, 1976; Meltzer, 1984). Ridge tops on the sandstone hills are dry. Well-developed stands of green alder (*Alnus viridis*) are common on south-facing slopes and especially in riparian floodplains. Shrub willows (*Salix* spp.) are generally <30 cm tall in open tundra situations, but individuals >2 m tall occur on riparian floodplains and south-facing hill slopes. The areas between hills are a mix of wetlands and mesic tundra vegetation. The study area is extensively grazed in summer by reindeer herds belonging to the Yamal Nenetsy people.

Two study sites were established at Laborovaya. LA-1, loamy site (Fig. S3-5a), is located in a valley between two sandstone ridges. The tundra on moist silt-loam soils is dominated by dwarf-shrubs (*Betula nana, Vaccinium vitis-idaea,* and *V. uligin*osum), sedges (*Carex bigelowii,* and *Eriophorum vaginatum*), and mosses (*Aulacomnium palustre, Hylocomium splendens,* and *Dicranum* spp.)

LA-2, sandy site (Fig. S3-5b), is on a younger (somewhat drier sandy terrace of a small stream with tundra consisting mainly of dwarf shrubs (*Betula nana, Vaccinium vitis-idaea,* and *V. uliginosum*) and lichens (*Cladonia arbuscula* and *Sphaerophorus globosus*).

Nadym

a. b.

Figure S3-6. Vegetation of the Nadym EAT study location. a. ND-1, sandy forest site. The trees are mainly Scots pine (*Pinus sylvestris*), and mountain birch (*Betula tortuosa*) mixed with Siberian larch (*Larix sibirica*). The understory consists of dwarf shrubs (*Rhododendron tomentosum, Betula nana, Empetrum nigrum, Vaccinium uliginosum,* and *V. vitis-idaea*), lichens (mainly *Cladonia stellaris*) and mosses (mainly *Pleurozium schreberi*). (Photo: P. Kuss). **b.** ND-2, loamy tundra site. Hummocky tundra consists of a complex of vegetation with a *Rhododendron tomentosum-Betula nana-Cladonia* spp. dwarf-shrub community on the hummocks and a *Cladonia stellaris-Carex glomerata* lichen community in the inter-hummock areas. (Photo: D.A. Walker.)

The southernmost EAT location (65˚ 19' N, 72˚ 53' E) is about 30 km south-southeast of the city of Nadym, in the forest-tundra transition of the Boreal bioclimate zone. The climate is influenced by maritime air masses from the Atlantic Ocean and continental air masses from central Asia. The mean annual temperature is -5.9 ˚C; the mean July temperature is 15.8 ˚C, and the mean SWI_g is 41.3 ˚C mo. Mean annual precipitation is 478 mm with over half of the total (252 mm) occurring during the summer (June-August). This is the only EAT location in the discontinuous permafrost zone; all others are in the continuous permafrost zone (Brown, Ferrians, Heginbottom, & Melnikov, 1997). It is also the only EAT location with forests and the only location along the mainland portion of the EAT that is not heavily grazed by reindeer, mainly because the local network of oilfield infrastructure limits access by herders and their animals. This is a long-term study area of Natalia Moskalenko and other researchers from the Earth Crysophere Institute (Melnikov, Leibman, Moskalenko, & Vasiliev, 2004; Moskalenko, 2003; 2007).

Two study sites were examined: ND-1, loamy, forest site (Fig. S3-6a) is on a lower and relatively young (about 20–40 ka BP) terrace of the Nadym River with no peat or permafrost. The vegetation at ND-1 is open birch-pine (*Pinus sylvestris* and *Betula tortuosa*) woodland with a dwarf-shrub and lichen understory (*Betula nana, Rhododendron tomentosum,* and *Cladonia stellaris*).

ND-2, sandy tundra site (Fig. S3-6b), is on a higher and relatively old (60–80 ka BP) fluvial-lacustrine plain. The vegetation at ND-2 consists of hummocky tundra with a complex of two dominant plant communities. A dwarf-shrub and lichen community (*Rhododendron tomentosum, Betula nana,* and *Cladonia* spp.) occurs on the tops of small earth hummocks and a lichen community (*Cladonia stellaris,* and *Carex glomerata*) occurs in the inter-hummock areas (Moskalenko, 2008). The ND-2 study plots were located around the margins of the Nadym, West

Siberia 100 x 100-m Circumpolar Active Layer Monitoring (CALM) grid to avoid disturbance to the central monitoring areas of the grid.

Literature cited

Alexandrova, V. D. (1980). The Arctic and Antarctic: Their Division into Geobotanical Areas. Cambridge: Cambridge University Press.

Brown, J., Ferrians, O. J., Heginbottom, J. A., & Melnikov, E. S. (1997). *Circum-Arctic Map of Permafrost and Ground-Ice Conditions*. *U.S. Geological Survey*. U.S. Geological Survey Map CP-45.

CAVM Team, Gould, W. A., Bliss, L. C., Edlund, S. A., Raynolds, M. K., Zoltai, S. C., et al. (2003). Circumpolar Arctic Vegetation Map. *Conservation of Arctic Flora and Fauna Map (CAFF) Map No. 1*. Anchorage, AK: U.S. Fish and Wildlife Service.

Dibner, V. D. (1965). The history of late Pleistocene and Holocene sedimentation in Franz Josef Land (in Russian). *Transactions of the Scientific Research Institute of the Geology of the Arctic*, *143*, 300–318.

Ermokhina, K. A. (2009). *Phytoindication of exogenic processes in Central Yamal tundra*. Moscow University, Moscow.

Forbes, B. C. (1997). Tundra disturbance studies IV. Species establishment on anthropogenic primary surfaces, Yamal Peninsula, Northwest Siberia, Russia. *Polar Geography*, *21*(1), 79–100.

Forbes, B. C. (2013). Cultural resilience of social-ecological systems in the Nenets and Yamal-Nenets Autonomous Okrugs, Russia: a focus on reindeer nomads of the tundra. *Ecology and Society*, *18*(4), art36. http://doi.org/10.5751/ES-05791-180436

Forman, S. L., Lubinski, D. J., Zeeberg, J. J., Snyder, J. A., Siegert, M. J., & Matishov, G. G. (2004). A review of postglacial emergence on Svalbard, Franz Josef Land and Novaya Zemlya, northern Eurasia. *Quaternary Science Reviews*, *23*(11-13), 1391–1434. http://doi.org/10.1016/j.quascirev.2003.12.007

Ilyina, I. S., Lapshina, E. I., Makhno, V. D., Meltzer, L. I., & Romanova, E. A. (1976). Vegetation of the West Siberian Plain, (1:1,500,000-scale map, 4 sheets). Moscow: State Cartography Press (GUGK).

Koryakin, Y. V., & Shipilov, E. V. (2009). Geochemical specifics and 40Ar/39Ar age of the basaltoid magmatism of the Alexander Land, Northbrook, Hooker and Hayes Islands (Franz Josef Land Archipelago) (In Russian). *Doklady Earth Sciences*, *425*, 260–263..

Kumpula, T., Forbes, B. C., Stammler, F., & Meschtyb, N. (2012). Dynamics of a coupled system: multi-resolution remote sensing in assessing social-ecological responses during 25 Years of gas field development in arctic Russia. *Remote Sensing*, *4*(4), 1046–1068. http://doi.org/10.3390/rs4041046

Leibman, M. O., Gubarkov, A. A., & Khomutov, A. V. (2012). Research Station Vaskiny Dachi: TICOP Excursion Guidebook: Tenth International Conference on Permafrost TICOP: Resources and risks of permafrost areas in a changing world (pp. 1–50). Tyumen: Pechatnik, Russia: North Press.

Leibman, M., Khomutov, A., Gubarkov, A., Mullanurov, D., & Dvornikov, Y. (2015). The research station "Vaskiny Dachi," Central Yamal, West Siberia, Russia - A review of 25 years of permafrost studies. *Fennia*, *193*, 3–30.

Lubinski, D. L., Forman, S. L., & Miller, G. H. (1999). Holocene glacier and climate fluctuations on Franz Josef Land, Arctic Russia, 80˚N. *Quaternary Science Reviews*, *18*, 85–108.

Makarova, O. L., Ermilov, S. G., Yurtaev, A. A., & Mansurov, R. I. (2015). The first data on the soil mites (Acari) of the Arctic Belyi Island (Northern Yamal, the Kara Sea). *Entomological Review*, *95*(6), 805–810. http://doi.org/10.1134/S0013873815060147

Melnikov, E. S., Leibman, M. O., Moskalenko, N. G., & Vasiliev, A. A. (2004). Active layer monitoring in West Siberia. *Polar Geography*, *28*(4), 284.

Meltzer, L. I. (1984). Zonal division of tundra vegetation of the West Siberian plain. (In Russian). In *Vegetation of western Siberia and its mapping* (pp. 7–19). Novosibirsk: Akademia Nauk.

Moskalenko, N. G. (2003). Interactions between vegetation and permafrost on some CALM grids in Russia (Vol. 2, pp. 789–794). Presented at the Permafrost: Proceedings of the Eighth International Conference on Permafrost, Zurich, Switzerland: A.A. Balkema Publishers.

Moskalenko, N. G. (2007). Impact of climate changes on West Siberia northern taiga ecosystems. (pp. 98–99). Presented at the Proceedings of the VIII International Symposium on Cold Region Development, Tampere, Finland.

Moskalenko, N. G. (2008). Overview of vegetation dynamics, disturbance and recovery studies in Nadym and Yamal areas. Presented at the Yamal Land-Cover Land-Use Change Workshop, Moscow, Russia.

Orekhov, P., Slagoda, E., & Popov, K. (2017). Factors of spatial differentiation of cryogenic geosystems of the Belyy Island Arctic tundras. Presented at the Arctic Science Summit Week, Prague, 31 Mar-07 Apr, Prague.

Rebristaya, O. V., & Khitun, O. V. (1998). Botanical-geographical features of the central Yamal flora. (In Russian). *Botanicheskii Zhurnal*, *83*(7), 37–52.

Rebristaya, O. V., (1995). Vascular plants of Belyy Island (Kara Sea). (In Russian). *Botanchisky Zhurnal*, *80*, 26–36.

Rebristaya, O. V., VV, K. O., Chernyadjeva, I. V., & Leibman, M. O. (1995). Dynamics of vegetation on the cryogenic landslips in the central part of the Yamal Peninsula. *Botanchisky Zhurnal*, *80*(4), 31–47.

Trofimov, V. T. (1975). Polustrov Yamal (Yamal Peninsula). (In Russian).Moscow: Moscow University Press.

Ukraintseva, N. G. (2008). Vegetation response to landslide spreading and climate change in the West SiberianTundra. In *Ninth International Conference on Permafrost* (pp. 1793–1798). Fairbanks.

Ukraintseva, N. G., Leibman, M. O., & Streletskaya, I. D. (2000). Peculiarities of landslide process in saline frozen deposits of central Yamal, Russia. In *Landslides. Proceedings VIII International Symposium on Landslides 3* (pp. 1495–1500). London: Thomas Telford.

Ukraintseva, N. G., Streletskaya, I. D., Ermokhina, K. A., & Yermakov, S. Y. (2003). Geochemical properties of plant-soil-permafrost system at landslide slopes, Yamal, Russia. In *Proceedings of the International Conference on Permafrost, Zurich, 21-25 July 2003* (Vol. II, pp. 1149–1154). Lisse, Nethrerlands: A.A. Balkema, Publishers.

Walker, D. A., Carlson, S., Frost, G. V., Matyshak, G. V., Leibman, M. E., Orechov, P., et al. (2011). *2010 Expedition to Krenkel Station, Hayes Island, Franz Josef Land Russia*. *AGC Data Report*. Fairbanks, AK: University of Alaska Fairbanks.

Walker, D. A., Epstein, H. E., Leibman, M. E., Moskalenko, N. G., Kuss, H. P., Matyshak, G. V., et al. (2008). *Data report of the 2007 Yamal expedition to Nadym, Laborovaya, and Vaskiny Dachi, Yamal Peninsula region, Russia*. *AGC Data Report*.

Walker, D. A., Epstein, H. E., Leibman, M. E., Moskalenko, N. G., Kuss, J. P., Matyshak, G. V., et al. (2009a). *Data Report of the 2007 and 2008 Yamal Expeditions: Nadym, Laborovaya, Vaskiny Dachi, and Kharasavey*. *AGC Data Report* (p. 133). Fairbanks, AK: University of Alaska.

Walker, D. A., Orekhov, P., Frost, G. V., Matyshak, G., Epstein, H. E., Leibman, M. O., et al. (2009b). *The 2009 Yamal Expedition to Ostrov Belyy and Kharp, Yamal Region, Russia*. *AGC Data Report* (p. 63). Fairbanks, AK: University of Alaska Fairbanks.

Washburn, A. L. (1980). Geocryology: A Survey of Periglacial Processes and Environments. New York: Halsted Press, John Wiley and Sons.

Yurtsev, B. A. (1994). The floristic division of the Arctic. *Journal of Vegetation Science*, *5*(6), 765–776.

Eurasia Arctic Transect species cover-abundance data

Appendix S4 is a tabular data file available for download at doi.org/10.1111/avsc.12401

Metadata:

Supplemental Information Appendix S4. Eurasia Arctic Transect species cover-abundance data.

Nomenclature for vascular plants follows the PanArctic Species List (Raynolds et al. 2013, CAFF Proceedings Series Report Nr. 10), which is a compiliation that includes the checklist for the vascular plants: Elven et al. 2007: Checklist of the Panarctic Flora (PAF). -Draft. University of Oslo.

Lichens followed H. Kristinsson & M. Zhurbenko 2006: Panarctic lichen checklist (http://archive.arcticportal.org/276/01/Panarctic_lichen_checklist.pdf).

Mosses followed M.S. Ignatov, O.M. Afonina & E.A. Ignatova 2006: Check-list of mosses of East Europe and North Asia. Arctoa 15: 1-130.

Liverworts followed N.A. Konstantinova & A.D. Potemkin 1996: Liverworts of Russian Arctic: an annotated check-list and bibliography. Arctoa 6: 125-150.

Cover-abundance scores: r = rare, + = <0.1% cover, 1 = 1-5%, 2 = 6-25%, 3 = 26-50% 4 = 51-75%, 5 = 76-100%.

Key to Plant Growth Form Codes is at the bottom of the table.

aava_eat_dwalker_2011_spp_modsrc.xlsx

Dataset Title: Eurasia Arctic Transect

Dataset Author: Donald A. (Skip) Walker

Dataset Reference: Data report, Walker et al. 2011

Dataset Table: Modified Species Cover Data for the Eurasia Arctic Transect

Dataset Notes: This is the modified dataset standardized for entry into Turboveg. Original field data are in Table 11 Walker et al. (2011). Species cover classes are the old Braun-Blanquet cover-abundance scale (r (rare), + (common, but less than 1 percent), 1 (1 to 5 percent), 2 (6 to 25 percent), 3 (25 to 50 percent), 4 (51 to 75 percent), and 5 (76 to 100 percent). Taxa are listed in alphabetical order. Both the Panarctic Species List (PASL) and dataset author's determinations are listed. In two instances, taxa were lumped into a single taxon in the PASL: 1) Dicranum spadiceum (Dicranum spadiceum and Dicranum laevidens) and, 2) Unknown moss = in orig. Hypnum holmenii (Hypnum holmenii and Stereodon holmenii). See readme in the metadata folder for further information about these data.

Eurasia Arctic Transect, plot environmental data

Appendix S5.1 is a tabular data file available for download at doi.org/10.1111/avsc.12401

Table caption:

79 plots. All plots were square. Plots 49 to 58 are divided into microsite subplots: 49a-53a = nonsorted circle centers, 49b-53b= intercircle areas; 54a-58a = small nonsorted polygon centers, 53b-58b = small nonsorted polygon cracks. SWI - Summer Warmth Index is the sum of the monthly means above 0 _C, and correlates well with tundra plant growth. See environmental metadata sheet for codes and units of variables. 999 indicates missing data. Subzone FT - Forest Tundra

Table S5.1 Field codes for environmental variables, Eurasia Arctic Transect

Landforms (Code)
1 Hills (including kames and moraines)
2 Talus slope
3 Colluvial basin
4 Glaciofluvial and other fluvial terraces
5 Marine terrace
6 Floodplains
7 Drained lakes and flat lake margins
8 Abandoned point bars and sloughs
9 Estuary
10 Lake or pond
11 Stream
12 Sea bluff
13 Lake bluff
14 Stream bluff
15 Sand dunes
16 Beach
17 Disturbed
18 Alluvial plain/abandoned
19 Island
20 Plain - residual surface
21 Marine terrace

Surficial Geology/ Parent Material (Code)
1 Glacial tills
2 Glaciofluvial deposits
3 Active alluvial sands
4 Active alluvial gravels
5 Stabilized alluvium (sands & gravels)
6 Undifferentiated hill slope colluvium
7 Basin colluvium and organic deposits
8 Drained lake or lacustrine organic deposits
9 Lake or pond organic, sand, or silt
10 Undifferentiated sands
11 Undifferentiated clay
12 Roads and gravel pads
13 Loess
14 Fine sand
15 Marine sands
16 Marine clay

Surficial Geomorphology/ Periglacial features (Code)
1 Frost scars
2 Wetland hummocks
3 Turf hummocks
4 Gelifluction features
5 Strangmoor or aligned hummocks
6 High- or flat-centered polygons
7 Mixed high- and low-centered polygons
8 Sorted and non-sorted stripes
9 Palsas
10 Thermokarst pits
11 Featureless or with less 20% frost scars
12 Well-developed hillslope water tracks and small streams > 50 cm deep
13 Poorly developed hillslope water tracks, < 50 cm deep
14 Gently rolling or irregular microrelief
15 Stoney surface
16 Lakes and ponds
17 Disturbed
18 Hillslope hummocks
19 Wetland
20 Small non-sorted polygon

Microsites (Code)
1 Frost-scar element
2 Inter-frost scar element
3 Strang or hummock
4 Flark, interstrang, or interhummock area
5 Polygon center
6 Polygon trough
7 Polygon rim
8 Stripe element
9 Inter-stripe element
10 Point bar (raised element)
11 Slough (wet element)
12 Raised ring of non-sorted circle
13 Thermokarst pit
14 Tops of small non-sorted polygons
15 Cracks between small non-sorted polygons

Site Moisture (modified from Komárková 1983) (Scalar)
1 Extremely xeric - almost no moisture; no plant growth
2 Very xeric - very little moisture; dry sand dunes
3 Xeric - little moisture; stabilized sand dunes, dry ridge tops
4 Subxeric - noticeable moisture; well-drained slopes, ridges
5 Subxeric to mesic - very noticeable moisture; flat to gently sloping
6 Mesic-moderate moisture; flat or shallow depressions
7 Mesic to subhygric - considerable moisture; depressions
8 Subhygric - very considerable moisture; saturated but with < 5% standing water < 10 cm deep
9 Hygric - much moisture; up to 100% of surface under water 10 to 50 cm deep; lake margins, shallow ponds, streams
10 Hydric - very much moisture; 100% of surface under water 50 to 150 cm deep; lakes, streams

Soil Moisture (from Komárková 1983) (Scalar)
1 Very dry - very little moisture; soil does not stick together
2 Dry - little moisture; soil somewhat sticks together
3 Damp - noticeable moisture; soil sticks together but crumbles
4 Damp to moist - very noticeable moisture; soil clumps
5 Moist - moderate moisture; soil binds but can be broken apart
6 Moist to wet - considerable moisture; soil binds and sticks to fingers
7 Wet - very considerable moisture; water drops can be squeezed out of soil
8 Very wet - much moisture can be squeezed out of soil
9 Saturated - very much moisture; water drips out of soil
10 Very saturated - extreme moisture; soil is more liquid than solid

Topographic Position (Code)
1 Hill crest or shoulder
2 Side slope
3 Footslope or toeslope
4 Flat
5 Drainage channel
6 Depression
7 Lake or pond

Estimated Snow Duration (Scalar)
1 Snow free all year
2 Snow free most of winter; some snow cover persists after storm but is blown free soon after
3 Snow free prior to melt out but with snow most of winter
4 Snow free immediately after melt out
5 Snow bank persists 1-2 weeks after melt out
6 Snow bank persists 3-4 weeks after melt out
7 Snow bank persists 4-8 weeks after melt out
8 Snow bank persists 8-12 weeks after melt out
9 Very short snow free period
10 Deep snow all year

Animal and Human Disturbance (degree) (Scalar)
0 No sign present
1 Some sign present; no disturbance
2 Minor disturbance or extensive sign
3 Moderate disturbance; small dens or light grazing
4 Major disturbance; multiple dens or noticeable trampling
5 Very major disturbance; very extensive tunneling or large pit

Animal and Human Disturbance (type) (Code)
1 Ptarmigan scat
2 Caribou tracks
3 Caribou scat
4 Goose tracks, scat, grazing
5 Squirrel mounds
6 Vole tracks & scat
7 Vehicle tracks
8 Fox seat

Stability (Scalar)
1 Stable
2 Subject to occasional disturbance
3 Subject to prolonged but slow disturbance such as solifluction
4 Annually disturbed
5 Disturbed more than once annually

Exposure Scale (Scalar)
1 Protected from winds
2 Moderate exposure to winds
3 Exposed to winds
4 Very exposed to winds

Texture (USDA Soil Survey) (Code)
1 Sand
2 Loamy sand
3 Sandy loam
4 Sandy clay loam
5 Sandy clay
6 Loam
7 Clay loam
8 Clay
9 Silty clay
10 Silty clay loam
11 Silt loam
12 Silt
13 Peat

Full synoptic table for statistical clusters of mesic tundra vegetation plots along the Eurasia Arctic Transect

Values are frequency of the given plant taxon within the indicated cluster (see Fig. 3, main text). Fidelity of diagnostic species was calculated using the phi coefficient (Chytrý et al. 2002) for individual clusters compared to the full suite of clusters. Diagnostic taxa are ordered according to descending fidelity (modified phi values). Taxa with very high fidelity (modified phi ≥ 0.8) have frequency values highlighted in dark gray; those with high fidelity (modified phi > 50) are highlighted in light gray. The second column in the table contains the plant growth form for each species: **bl**, bryophyte, liverwort; **bma**, bryophyte, moss, acrocarpous; **bmp**, bryophyte, moss, pleurocarpous; **bms**, bryophyte, moss, sphagnoid; **fe**, forb, erect; **fm**, forb, mat, cushion or rosette; **gs**, graminoid, sedge; **gg**, graminoid, grass; **gr**, graminoid, rush; **lc**, lichen, crustose; **lfo**, lichen, foliose; **lfr**, lichen, fruticose; **sle**, shrub, low, evergreen; **sld**, shrub, low, deciduous; **sde**, shrub, dwarf, evergreen; **sdd**, shrub, dwarf, deciduous; **tne**, tree, needleleaf, evergreen; **tnd**, tree, needleleaf, deciduous; **tbd**, tree, broadleaf, deciduous; **vs**, vascular plant, seedless.

Cluster nr.		**1**	**2**	**4**	**5**	**6**	**7**	**3**
Subzone(s) (soil texture)		**FT(lom)**	**FT(snd)**	**E+D(snd)**	**D(lom)+C**	**B(lom)**	**B(snd)**	**A**
Nr of relevés		**5**	**6**	**15**	**20**	**10**	**10**	**10**
Diagnostic taxa for cluster 1:	**Growth form**							
Pinus sylvestris	tne	100	.	.	.	.	.	.
Betula pubescens	tbd	100	.	.	.	.	.	.
Larix sibirica	tnd	100	.	.	.	.	.	.
Vaccinium myrtillus	sdd	100	.	.	.	.	.	.
Juniperus communis	sle	80	.	.	.	.	.	.
Peltigera malacea	lfo	60	.	.	.	.	.	.
Pleurozium schreberi	bmp	100	17	47	5	.	.	.
Peltigera leucophlebia	lfo	100	.	13	50	20	.	.
Cladonia stellaris	lfr	100	83	20	.	.	.	.
Empetrum nigrum	sde	100	17	80	10	.	.	.
Vaccinium uliginosum	sdd	100	33	67	15	.	.	.
Diagnostic taxa for cluster 2;								
Carex globularis	gs	.	100	.	.	.	.	.
Andromeda polifolia	sde	.	83	7	.	.	.	.
Rubus chamaemorus	sdd	.	83	7	.	.	.	.
Rhododendron tomentosum s. *tomentosum*	sle	100	100	73	.	.	.	.
Diagnostic taxa for cluster 4:								
Flavocetraria nivalis	lfr	.	.	93	25	.	.	.
Salix phylicifolia	sld	.	.	67	10	.	.	.
Eriophorum vaginatum	gs	.	17	87	25	.	.	.
Pedicularis labradorica	fe	.	.	53	.	.	.	.
Asahinea chrysantha	lfr	.	.	40	.	.	.	.
Pertusaria dactylina	lc	.	.	47	.	.	10	.
Cladonia grayi	lfr	.	.	40	5	.	.	.

Cluster nr.		1	2	4	5	6	7	3
Subzone(s) (soil texture)		**FT(lom)**	**FT(snd)**	**E+D(snd)**	**D(lom)+C**	**B(lom)**	**B(snd)**	**A**
Nr of relevés		**5**	**6**	**15**	**20**	**10**	**10**	**10**
Schljakovia kunzeana	bl	.	.	33	.	.	.	.
Luzula wahlenbergii	gr	.	.	33	.	.	.	.
Diagnostic taxon for clusters 5 & 6:								
Arctagrostis latifolia	gg	.	.	20	95	100	10	.
Diagnostic taxa for cluster 5:								
Lophozia ventricosa	bl	.	.	40	80	.	.	.
Alopecurus borealis	gg	.	.	.	60	.	.	10
Salix reptans	sdd	.	.	13	55	.	.	.
Eriophorum angustifolium	gs	.	.	27	60	.	.	.
Tephroseris atropurpurea	fe	.	.	7	45	.	.	.
Peltigera canina	lfo	.	.	.	35	.	.	.
Peltigera aphthosa	lfo	.	.	.	40	10	.	.
Lichenomphalia hudsoniana	lfo	.	.	.	30	.	.	.
Diagnostic taxa for cluster 6:								
Blepharostoma trichophyllum	bl	.	.	.	5	100	.	.
Salix polaris	sdd	.	.	.	50	100	.	.
Tomentypnum nitens	bmp	.	.	13	20	90	.	.
Dryas octopetala	sde	.	.	.	40	100	50	.
Poa arctica	gg	.	.	7	40	80	.	.
Juncus biglumis	gr	.	.	.	.	60	20	.
Bryum cyclophyllum	bma	.	.	.	.	40	.	.
Stellaria longipes	fe	.	.	.	25	60	.	.
Sphenolobus minutus	bl	.	.	73	80	100	20	.
Diagnostic taxa for cluster 7:								
Pogonatum dentatum	bma	.	.	13	.	.	80	.
Oxyria digyna	fm	.	.	.	.	.	80	20
Gymnomitrion corallioides	bl	.	.	33	25	10	100	.
Luzula confusa	gr	.	.	.	60	10	100	.
Salix nummularia	sdd	.	.	27	50	.	100	.
Lloydia serotina	fe	.	.	.	.	.	50	.
Solorina crocea	lfo	.	.	.	.	.	50	.
Polytrichum piliferum	bma	.	.	7	.	10	50	.
Pohlia crudoides	bma	.	.	7	.	.	40	.
Gowardia nigricans	lfr	.	.	40	60	20	90	.
Diagnostic taxa for cluster 3:								
Stellaria longipes taxon edwardsii	fe	.	.	.	.	.	.	100
Papaver dahlianum agg. (*P. cornwallisense*)	fm	.	.	.	.	.	.	100

Cluster nr.		1	2	4	5	6	7	3
Subzone(s) (soil texture)		FT(lom)	FT(snd)	E+D(snd)	D(lom)+C	B(lom)	B(snd)	A
Nr of relevés		5	6	15	20	10	10	10
Phippsia algida	gg	.	.	.	.	.	.	100
Cochlearia groenlandica	fm	.	.	.	.	.	.	100
Lecidea ramulosa	lc	.	.	.	.	.	.	100
Orthothecium chryseum	bmp	.	.	.	.	10	.	100
Cladonia pocillum	lfr	.	.	.	.	10	.	100
Cetrariella delisei	lfr	.	.	20	.	.	.	100
Cerastium nigrescens v. *laxum*	fm	.	.	.	.	.	.	80
Fulgensia bracteata	lc	.	.	.	.	.	.	80
Saxifraga cernua	fe	.	.	.	5	.	.	80
Draba subcapitata	fm	.	.	.	.	.	20	90
Cirriphyllum cirrosum	bmp	.	.	.	.	.	.	70
Cerastium regelii	fm	.	.	.	.	10	.	70
Encalypta alpina	bma	.	.	.	.	.	.	60
Solorina bispora	lfo	.	.	.	.	.	.	60
Bryum rutilans	bma	.	.	.	.	.	.	60
Saxifraga cespitosa	fm	.	.	.	.	.	.	60
Distichium capillaceum	bma	.	.	.	.	30	.	80
Cetraria aculeata	lfr	.	.	.	.	.	20	70
Pohlia cruda	bma	.	.	.	.	40	.	80
Gowardia arctica	lfr	.	.	.	.	.	.	50
Saxifraga oppositifolia	fm	.	.	.	.	.	.	50
Cladonia symphycarpia	lfr	.	.	.	.	.	.	50
Stereocaulon rivulorum	lfr	.	.	.	.	.	.	50
Polytrichastrum alpinum	bma	.	.	.	30	10	60	100
Bartramia ithyphylla	bma	.	.	.	.	.	10	50
Callialaria curvicaulis	bmp	.	.	.	.	.	.	40
Campylium stellatum v. *arcticum*	bmp	.	.	.	.	.	.	40
Ditrichum flexicaule	bma	.	.	.	5	40	.	70
Protopannaria pezizoides	lc	.	.	.	5	.	.	40
Nondiagnostic taxa occuring in more than one cluster:								
Cladonia stygia	lfr	60	100	93	60	.	.	.
Betula nana	sld	100	50	80	45	.	.	.
Dicranum fuscescens	bma	40	17	20	15	.	.	.
Cladonia cornuta	lfr	20	17	33	20	.	.	.
Polytrichum commune	bma	60	.	20	5	.	.	.
Festuca ovina [s. ovina]	gg	20	.	27	30	.	.	.
Peltigera neckeri	lfo	20	.	27	5	.	.	.

Cluster nr.		1	2	4	5	6	7	3
Subzone(s) (soil texture)		FT(lom)	FT(snd)	E+D(snd)	D(lom)+C	B(lom)	B(snd)	A
Nr of relevés		5	6	15	20	10	10	10
Cetraria islandica	lfr	100	33	100	100	100	60	100
Cladonia arbuscula s. lat.	lfr	60	17	93	75	100	30	.
Cladonia rangiferina	lfr	60	17	60	50	90	30	.
Ptilidium ciliare	bl	20	17	100	60	90	10	.
Polytrichum strictum	bma	20	50	73	50	100	70	.
Dicranum acutifolium	bma	20	17	20	35	70	20	.
Peltigera scabrosa	lfo	20	.	33	60	40	10	.
Cladonia gracilis s. lat.	lfr	20	.	67	95	90	60	.
Vaccinium vitis-idaea	sde	100	100	87	60	.	20	.
Flavocetraria cucullata	lfr	.	50	100	100	40	20	100
Cetraria laevigata	lfr	.	67	20	10	20	.	.
Cladonia amaurocraea	lfr	.	100	80	90	100	20	.
Cladonia coccifera s. lat.	lfr	.	50	93	90	100	70	.
Pohlia nutans	bma	.	33	40	45	40	30	.
Dicranum elongatum	bma	.	33	87	95	100	50	.
Cladonia deformis	lfr	.	33	13	20	.	.	.
Aulacomnium turgidum	bmp	.	17	87	100	100	20	.
Cladonia bellidiflora	lfr	.	17	60	40	.	20	.
Ptilium crista-castrensis	bmp	.	17	7	.	.	.	.
Polytrichum jensenii	bma	.	17	13	.	.	.	.
Cladonia sulphurina	lfr	.	33	13	5	.	.	.
Cladonia macrophylla	lfr	.	17	7	5	.	.	.
Pedicularis lapponica	fe	.	.	33	5	.	.	.
Polytrichum hyperboreum	bma	.	.	33	15	.	.	.
Hierochloë alpina	gg	.	.	27	20	.	.	.
Cladonia squamosa s. lat.	lfr	.	.	27	15	.	.	.
Pertusaria geminipara	lc	.	.	20	5	.	.	.
Cladonia cenotea	lfr	.	.	13	5	.	.	.
Valeriana capitata	fe	.	.	7	20	.	.	.
Orthocaulis binsteadii	bl	.	.	7	20	.	.	.
Calliergon stramineum	bmp	.	.	7	5	.	.	.
Sphagnum girgensohnii	bms	.	.	7	5	.	.	.
Arctocetraria andrejevii	lfr	.	.	7	10	.	.	.
Peltigera frippii	lfo	.	.	7	10	.	.	.
Ceratodon purpureus	bma	.	.	7	10	.	.	.
Salix hastata	sld	.	.	7	20	.	.	.
Cladonia chlorophaea	lfr	.	.	7	30	.	.	.

Cluster nr.		1	2	4	5	6	7	3
Subzone(s) (soil texture)		FT(lom)	FT(snd)	E+D(snd)	D(lom)+C	B(lom)	B(snd)	A
Nr of relevés		5	6	15	20	10	10	10
Carex bigelowii	gs	.	.	100	100	100	.	.
Oncophorus wahlenbergii	bma	.	.	13	10	50	.	.
Psoroma hypnorum	lc	.	.	13	20	40	.	.
Tritomaria quinquedentata	bl	.	.	7	45	60	.	.
Dactylina arctica	lfr	.	.	93	100	80	40	.
Sphaerophorus globosus	lfr	.	.	93	95	100	100	.
Cladonia uncialis	lfr	.	.	87	75	100	60	.
Calamagrostis holmii	gg	.	.	87	95	100	40	.
Cladonia subfurcata	lfr	.	.	80	60	50	40	.
Racomitrium lanuginosum	bmp	.	.	73	70	50	90	.
Hylocomium splendens	bmp	.	.	67	100	100	50	.
Dicranum spadiceum	bma	.	.	53	70	20	20	.
Bryoria nitidula	lfr	.	.	33	5	10	40	.
Cladonia stricta s. lat.	lfr	.	.	20	10	10	10	.
Cetrariella fastigiata	lfr	.	.	13	10	20	10	.
Alectoria ochroleuca	lfr	.	.	53	35	.	60	.
Pertusaria panyrga	lc	.	.	13	5	.	20	.
Aulacomnium palustre	bmp	.	.	20	20	.	10	.
Bistorta vivipara	fe	.	.	7	40	.	40	.
Conostomum tetragonum	bma	.	.	27	.	20	20	.
Ochrolechia inaequatula	lc	.	.	13	65	30	.	30
Thamnolia vermicularis	lfr	.	.	100	100	100	100	100
Bryocaulon divergens	lfr	.	.	80	85	50	100	40
Sanionia uncinata	bmp	.	.	33	40	70	10	20
Stereocaulon alpinum	lfr	.	.	33	40	20	20	70
Ochrolechia frigida	lc	.	.	100	25	90	100	10
Cladonia pyxidata	lfr	.	.	20	20	40	.	10
Pogonatum urnigerum	bma	.	.	7	.	.	.	20
Baeomyces rufus	lfr	.	.	7	.	.	.	10
Lobaria linita	lfo	.	.	.	30	50	.	.
Tetraplodon mnioides	bma	.	.	.	5	10	.	.
Micranthes foliolosa	fm	.	.	.	5	10	.	.
Eriophorum scheuchzeri	gs	.	.	.	5	30	.	.
Nephroma expallidum	lfo	.	.	.	5	20	.	.
Luzula nivalis	gr	.	.	.	5	30	.	.
Pedicularis hirsuta	fe	.	.	.	40	.	60	.
Parmelia omphalodes s. lat.	lfo	.	.	.	35	50	60	10

Cluster nr.		1	2	4	5	6	7	3
Subzone(s) (soil texture)		**FT(lom)**	**FT(snd)**	**E+D(snd)**	**D(lom)+C**	**B(lom)**	**B(snd)**	**A**
Nr of relevés		**5**	**6**	**15**	**20**	**10**	**10**	**10**
Sagina nivalis	fm	.	.	.	.	20	10	.
Dactylina ramulosa	lfr	.	.	.	.	20	10	.
Anthelia juratzkana	bl	.	.	.	.	50	.	40
Bryoerythrophyllum recurvirostre	bma	.	.	.	.	30	.	50
Bryum pseudotriquetrum	bma	.	.	.	.	20	.	30
	Nondiagnostic taxa occurring in only one cluster:							
Pinus sibirica	tne	40	.	.	.	.	.	.
Polytrichum longisetum	bma	20	.	.	.	.	.	.
Diphasiastrum alpinum	vs	20	.	.	.	.	.	.
Sphagnum fuscum	bms	.	33	.	.	.	.	.
Mylia anomala	bl	.	33	.	.	.	.	.
Calypogeia sphagnicola	bl	.	17	.	.	.	.	.
Drosera rotundifolia	fm	.	17	.	.	.	.	.
Kiaeria blyttii	bma	.	17	.	.	.	.	.
Oxycoccus microcarpus	sde	.	17	.	.	.	.	.
Protothelenella leucothelia	lc	.	17	.	.	.	.	.
Cladonia crispata s. lat.	lfr	.	17	.	.	.	.	.
Icmadophila ericetorum	lc	.	.	27	.	.	.	.
Petasites frigidus	fe	.	.	27	.	.	.	.
Hypogymnia physodes	lfo	.	.	20	.	.	.	.
Arctous alpina	sdd	.	.	20	.	.	.	.
Dicranum groenlandicum	bma	.	.	13	.	.	.	.
Huperzia selago	vs	.	.	13	.	.	.	.
Minuartia arctica	fm	.	.	13	.	.	.	.
Stereocaulon paschale	lfr	.	.	13	.	.	.	.
Varicellaria rhodocarpa	lc	.	.	13	.	.	.	.
Gymnocolea inflata	bl	.	.	13	.	.	.	.
Sphagnum rubellum	bms	.	.	13	.	.	.	.
Diapensia lapponica	fm	.	.	13	.	.	.	.
Sphagnum balticum	bms	.	.	13	.	.	.	.
Sphagnum lenense	bms	.	.	13	.	.	.	.
Sphagnum teres	bms	.	.	7	.	.	.	.
Cynodontium strumiferum	bma	.	.	7	.	.	.	.
Sphagnum warnstorfii	bms	.	.	7	.	.	.	.
Cetraria nigricans	lfr	.	.	7	.	.	.	.
Ochrolechia androgyna	lc	.	.	7	.	.	.	.
Carex rotundata	gs	.	.	7	.	.	.	.

Cluster nr.		1	2	4	5	6	7	3
Subzone(s) (soil texture)		FT(lom)	FT(snd)	E+D(snd)	D(lom)+C	B(lom)	B(snd)	A
Nr of relevés		5	6	15	20	10	10	10
Salix myrtilloides	sld	.	.	7	.	.	.	.
Sphagnum squarrosum	bms	.	.	7	.	.	.	.
Tetralophozia setiformis	bl	.	.	7	.	.	.	.
Peltigera polydactylon	lfo	.	.	7	.	.	.	.
Sphagnum majus	bms	.	.	7	.	.	.	.
Deschampsia sukatschewii	gg	.	.	.	15	.	.	.
Cladonia decorticata	lfr	.	.	.	10	.	.	.
Plagiomnium ellipticum	bma	.	.	.	10	.	.	.
Protomicarea limosa	lc	.	.	.	10	.	.	.
Dicranella subulata	bma	.	.	.	10	.	.	.
Cladonia pleurota	lfr	.	.	.	10	.	.	.
Peltigera kristinssonii	lfo	.	.	.	10	.	.	.
Splachnum sphaericum	bma	.	.	.	10	.	.	.
Plagiothecium berggrenianum	bmp	.	.	.	10	.	.	.
Rinodina turfacea	lc	.	.	.	10	.	.	.
Rumex arcticus	fe	.	.	.	10	.	.	.
Cladonia scabriuscula	lfr	.	.	.	5	.	.	.
Japewia tornoënsis	lc	.	.	.	5	.	.	.
Dicranum majus	bma	.	.	.	5	.	.	.
Polemonium acutiflorum	fe	.	.	.	5	.	.	.
Pachypleurum alpinum	fe	.	.	.	5	.	.	.
Parrya nudicaulis	fe	.	.	.	5	.	.	.
Trisetum spicatum	gg	.	.	.	5	.	.	.
Warnstorfia pseudostraminea	bmp	.	.	.	5	.	.	.
Carex aquatilis	gs	.	.	.	5	.	.	.
Abietinella abietina	bmp	.	.	.	5	.	.	.
Rhexophiale rhexoblephara	lc	.	.	.	5	.	.	.
Hypnum subimponens	bmp	.	.	.	5	.	.	.
Cladonia cyanipes	lfr	.	.	.	5	.	.	.
Salix lanata	sld	.	.	.	5	.	.	.
Aplodon wormskjoldii	bma	.	.	.	5	.	.	.
Sticta arctica	lfo	.	.	.	.	30	.	.
Bacidia bagliettoana	lc	.	.	.	.	20	.	.
Micarea incrassata	lc	.	.	.	.	20	.	.
Myurella tenerrima	bmp	.	.	.	.	20	.	.
Meesia uliginosa	bma	.	.	.	.	20	.	.
Hypogymnia subobscura	lfo	.	.	.	.	20	.	.

Cluster nr.		1	2	4	5	6	7	3
Subzone(s) (soil texture)		**FT(lom)**	**FT(snd)**	**E+D(snd)**	**D(lom)+C**	**B(lom)**	**B(snd)**	**A**
Nr of relevés		**5**	**6**	**15**	**20**	**10**	**10**	**10**
Arctocetraria nigricascens	lfr	.	.	.	.	10	.	.
Orthothecium strictum	bmp	.	.	.	.	10	.	.
Warnstorfia sarmentosa	bmp	.	.	.	.	10	.	.
Cephalozia bicuspidata	bl	.	.	.	.	10	.	.
Tortella fragilis	bma	.	.	.	.	10	.	.
Splachnum vasculosum	bma	.	.	.	.	10	.	.
Oncophorus compactus	bma	.	.	.	.	10	.	.
Potentilla hyparctica	fm	.	.	.	.	.	20	.
Micranthes tenuis	fm	.	.	.	.	.	10	.
Siphula ceratites	lfr	.	.	.	.	.	10	.
Lecanora geophila	lc	.	.	.	.	.	.	30
Candelariella placodizans	lc	.	.	.	.	.	.	30
Myurella julacea	bmp	.	.	.	.	.	.	30
Racomitrium panschii	bmp	.	.	.	.	.	.	30
Oncophorus virens	bma	.	.	.	.	.	.	30
Lepraria gelida	lc	.	.	.	.	.	.	20
Peltigera venosa	lfo	.	.	.	.	.	.	10
Cerastium arcticum	fm	.	.	.	.	.	.	10
Sanionia nivalis	bmp	.	.	.	.	.	.	10
Hypnum revolutum	bmp	.	.	.	.	.	.	10
Physconia muscigena	lfo	.	.	.	.	.	.	10
Syntrichia ruralis	bma	.	.	.	.	.	.	10
Psilopilum cavifolium	bma	.	.	.	.	.	.	10

Diagnostic (Dg), constant (C), and dominant (Dm) taxa in each numerical cluster (Fig. 3 of main text) used in analysis of the Eurasia Arctic Transect vegetation plot data

Determination of diagnostic, constant, and dominant species was determined at two threshold levels. Bolded species are those with the higher threshold values for diagnostic species (fidelity, phi values) and constant species (frequency occurrence). Threshold fidelity values were: diagnostic species (phi values); 50 (**80**); constant species (% frequency): 40 (**50**); dominant species (% with cover >25%).

Cluster 1
Number of relevés: 5

Diagnostic species: ***Vaccinium myrtillus (C) 100.0, Pinus sylvestris (C) 100.0, Larix sibirica (C) 100.0, Betula pubescens (C) 100.0, Juniperus communis (C) 88.0,*** *Peltigera malacea (C) 75.0, Pleurozium schreberi (C, Dm) 72.6, Peltigera leucophlebia (C) 68.5, Cladonia stellaris (C, Dm) 63.8, Empetrum nigrum (C) 63.1, Vaccinium uliginosum (C) 61.3*

Constant species: ***Vaccinium vitis-idaea 100, Vaccinium uliginosum (Dg) 100, Vaccinium myrtillus (Dg) 100, Rhododendron tomentosum s. tomentosum 100, Pleurozium schreberi (Dg, Dm) 100, Pinus sylvestris (Dg) 100, Peltigera leucophlebia (Dg) 100, Larix sibirica (Dg) 100, Empetrum nigrum (Dg) 100, Cladonia stellaris (Dg, Dm) 100, Cetraria islandica 100, Betula pubescens (Dg) 100, Betula nana 100, Juniperus communis (Dg) 80, Polytrichum commune 60, Peltigera malacea (Dg) 60, Cladonia stygia 60, Cladonia rangiferina 60, Cladonia arbuscula s. lat. 60***

Dominant species: *Cladonia stellaris (Dg, C) 100, Pleurozium schreberi (Dg, C) 40*

Cluster 2
Number of relevés: 6

Diagnostic species: ***Carex globularis (C) 100.0, Rubus chamaemorus (C) 86.0, Andromeda polifolia (C) 86.0,*** *Rhododendron tomentosum s. tomentosum (C, Dm) 51.0*

Constant species: ***Vaccinium vitis-idaea 100, Rhododendron tomentosum s. tomentosum (Dg, Dm) 100, Cladonia stygia (Dm) 100, Cladonia amaurocraea 100, Carex globularis (Dg) 100, Rubus chamaemorus (Dg) 83, Cladonia stellaris (Dm) 83, Andromeda polifolia (Dg) 83, Cetraria laevigata 67,*** *Polytrichum strictum 50, Flavocetraria cucullata 50, Cladonia coccifera s. lat. 50, Betula nana 50*

Dominant species: *Cladonia stellaris (C) 67, Rhododendron tomentosum s. tomentosum (Dg, C) 50, Sphagnum fuscum 17, Cladonia stygia (C) 17*

Cluster 3
Number of relevés: 10

Diagnostic species: ***Stellaria longipes taxon edwardsii (C) 100.0, Phippsia algida (C) 100.0, Papaver dahlianum agg. (P. cornwallisense) (C) 100.0, Lecidea ramulosa (C) 100.0, Cochlearia groenlandica (C) 100.0, Orthothecium chryseum (C) 94.5, Cladonia pocillum (C) 94.5, Cetrariella delisei (C) 89.8, Fulgensia bracteata (C) 88.0, Cerastium nigrescens v. laxum (C) 88.0, Saxifraga cernua (C) 84.8, Draba subcapitata (C) 83.3, Cirriphyllum cirrosum (C) 81.6,*** *Cerastium regelii (C) 75.2, Solorina bispora (C) 75.0, Saxifraga cespitosa (C) 75.0, Encalypta alpina (C) 75.0, Bryum rutilans (C) 75.0, Distichium capillaceum (C) 72.1, Cetraria aculeata (C) 69.7, Pohlia cruda (C) 68.1, Stereocaulon rivulorum (C) 67.9, Saxifraga oppositifolia (C) 67.9, Gowardia arctica (C) 67.9, Cladonia symphycarpia (C) 67.9, Polytrichastrum alpinum (C) 64.5, Bartramia ithyphylla (C) 60.4, Polytrichastrum alpinum v. fragile 60.3, Campylium stellatum v. arcticum 60.3, Callialaria curvicaulis 60.3, Ditrichum flexicaule (C) 59.0, Protopannaria pezizoides 55.9*

Constant species: ***Thamnolia vermicularis 100, Stellaria longipes taxon edwardsii (Dg) 100, Polytrichastrum alpinum (Dg) 100, Phippsia algida (Dg) 100, Papaver dahlianum agg. (P. cornwallisense) (Dg) 100, Orthothecium***

chryseum (Dg) 100, Lecidea ramulosa (Dg) 100, Flavocetraria cucullata 100, Cochlearia groenlandica (Dg) 100, Cladonia pocillum (Dg) 100, Cetrariella delisei (Dg) 100, Cetraria islandica 100, Draba subcapitata (Dg) 90, Saxifraga cernua (Dg) 80, Pohlia cruda (Dg) 80, Fulgensia bracteata (Dg) 80, Distichium capillaceum (Dg) 80, Cerastium nigrescens v. laxum (Dg) 80, Stereocaulon alpinum 70, Ditrichum flexicaule (Dg) 70, Cirriphyllum cirrosum (Dg) 70, Cetraria aculeata (Dg) 70, Cerastium regelii (Dg) 70, Solorina bispora (Dg) 60, Saxifraga cespitosa (Dg) 60, Encalypta alpina (Dg) 60, Bryum rutilans (Dg) 60, *Stereocaulon rivulorum (Dg) 50, Saxifraga oppositifolia (Dg) 50, Gowardia arctica (Dg) 50, Cladonia symphycarpia (Dg) 50, Bryoerythrophyllum recurvirostre 50, Bartramia ithyphylla (Dg) 50*

Dominant species: None

Cluster 4
Number of relevés: 15

Diagnostic species: ***Flavocetraria nivalis (C) 83.3,*** *Salix phylicifolia (C) 72.8, Eriophorum vaginatum (C) 72.1, Pedicularis labradorica (C) 70.3, Asahinea chrysantha 60.3, Pertusaria dactylina (C) 57.7, Cladonia grayi 55.9, Schljakovia kunzeana 54.8, Luzula wahlenbergii 54.8*

Constant species: ***Thamnolia vermicularis 100, Ptilidium ciliare 100, Ochrolechia frigida 100, Flavocetraria cucullata 100, Cetraria islandica 100, Carex bigelowii (Dm) 100, Sphaerophorus globosus (Dm) 93, Flavocetraria nivalis (Dg) 93, Dactylina arctica 93, Cladonia stygia 93, Cladonia coccifera s. lat. 93, Cladonia arbuscula s. lat. 93, Vaccinium vitis-idaea (Dm) 87, Eriophorum vaginatum (Dg) 87, Dicranum elongatum (Dm) 87, Cladonia uncialis 87, Calamagrostis holmii 87, Aulacomnium turgidum 87, Empetrum nigrum 80, Cladonia subfurcata 80, Cladonia amaurocraea 80, Bryocaulon divergens 80, Betula nana (Dm) 80, Sphenolobus minutus 73, Rhododendron tomentosum s. tomentosum 73, Racomitrium lanuginosum 73, Polytrichum strictum 73, Vaccinium uliginosum 67, Salix phylicifolia (Dg) 67, Hylocomium splendens 67, Cladonia gracilis s. lat. 67, Cladonia rangiferina 60, Cladonia bellidiflora 60, Pedicularis labradorica (Dg) 53, Dicranum spadiceum 53, Alectoria ochroleuca 53,*** *Pleurozium schreberi 47, Pertusaria dactylina (Dg) 47*

Dominant species: *Betula nana (C) 20, Sphaerophorus globosus (C) 13, Vaccinium vitis-idaea (C) 7, Dicranum elongatum (C) 7, Carex bigelowii (C) 7*

Cluster 5
Number of relevés: 20

Diagnostic species: *Lophozia ventricosa (C) 68.1, Alopecurus borealis (C) 68.0, Salix reptans (C) 62.2, Eriophorum angustifolium (C) 59.0, Tephroseris atropurpurea (C) 58.7, Peltigera canina 56.2, Arctagrostis latifolia (C) 54.9, Peltigera aphthosa 52.1, Lichenomphalia hudsoniana 51.8*

Constant species: ***Thamnolia vermicularis 100, Hylocomium splendens (Dm) 100, Flavocetraria cucullata 100, Dactylina arctica 100, Cetraria islandica 100, Carex bigelowii (Dm) 100, Aulacomnium turgidum (Dm) 100, Sphaerophorus globosus 95, Dicranum elongatum (Dm) 95, Cladonia gracilis s. lat. 95, Calamagrostis holmii (Dm) 95, Arctagrostis latifolia (Dg) 95, Cladonia coccifera s. lat. 90, Cladonia amaurocraea 90, Bryocaulon divergens 85, Sphenolobus minutus 80, Lophozia ventricosa (Dg) 80, Cladonia uncialis 75, Cladonia arbuscula s. lat. 75, Racomitrium lanuginosum 70, Dicranum spadiceum (Dm) 70, Ochrolechia inaequatula 65, Vaccinium vitis-idaea (Dm) 60, Ptilidium ciliare 60, Peltigera scabrosa 60, Luzula confusa 60, Gowardia nigricans 60, Eriophorum angustifolium (Dg) 60, Cladonia subfurcata 60, Cladonia stygia 60, Alopecurus borealis (Dg) 60, Salix reptans (Dg) 55,*** *Salix polaris (Dm) 50, Salix nummularia (Dm) 50, Polytrichum strictum (Dm) 50, Peltigera leucophlebia 50, Cladonia rangiferina 50, Tritomaria quinquedentata 45, Tephroseris atropurpurea (Dg) 45, Pohlia nutans 45, Betula nana (Dm) 45*

Dominant species: *Aulacomnium turgidum (C) 25, Hylocomium splendens (C) 20, Carex bigelowii (C) 20, Salix nummularia (C) 15, Betula nana (C) 10, Vaccinium vitis-idaea (C) 5, Salix polaris (C) 5, Polytrichum strictum (C) 5, Dicranum spadiceum (C) 5, Dicranum fuscescens 5, Dicranum elongatum (C) 5, Calamagrostis holmii (C) 5*

Cluster 6
Number of relevés: 10

Diagnostic species: ***Blepharostoma trichophyllum (C, Dm) 97.2,*** *Salix polaris (C, Dm) 78.2, Tomentypnum nitens (C) 77.6, Dryas octopetala (C) 66.9, Poa arctica (C) 65.6, Juncus biglumis (C) 62.3, Bryum cyclophyllum 60.3, Stellaria longipes (C) 59.8, Arctagrostis latifolia (C) 59.3, Sphenolobus minutus (C) 51.0*

Constant species: ***Thamnolia vermicularis 100, Sphenolobus minutus (Dg) 100, Sphaerophorus globosus 100, Salix polaris (Dg, Dm) 100, Polytrichum strictum 100, Hylocomium splendens (Dm) 100, Dryas octopetala (Dg) 100, Dicranum elongatum (Dm) 100, Cladonia uncialis 100, Cladonia coccifera s. lat. 100, Cladonia arbuscula s. lat. (Dm) 100, Cladonia amaurocraea 100, Cetraria islandica 100, Carex bigelowii (Dm) 100, Calamagrostis holmii 100, Blepharostoma trichophyllum (Dg, Dm) 100, Aulacomnium turgidum 100, Arctagrostis latifolia (Dg) 100, Tomentypnum nitens (Dg) 90, Ptilidium ciliare 90, Ochrolechia frigida 90, Cladonia rangiferina 90, Cladonia gracilis s. lat. 90, Poa arctica (Dg) 80, Dactylina arctica 80, Sanionia uncinata 70, Dicranum acutifolium 70, Tritomaria quinquedentata 60, Stellaria longipes (Dg) 60, Juncus biglumis (Dg) 60,*** *Racomitrium lanuginosum 50, Parmelia omphalodes s. lat. 50, Oncophorus wahlenbergii 50, Lobaria linita 50, Cladonia subfurcata 50, Bryocaulon divergens 50, Anthelia juratzkana 50*

Dominant species: *Salix polaris (Dg, C) 50, Carex bigelowii (C) 50, Hylocomium splendens (C) 40, Cladonia arbuscula s. lat. (C) 40, Dicranum elongatum (C) 10, Blepharostoma trichophyllum (Dg, C) 10*

Cluster 7

Diagnostic species: ***Pogonatum dentatum (C) 80.1,*** *Oxyria digyna (C) 76.7, Gymnomitrion corallioides (C, Dm) 72.6, Luzula confusa (C) 72.1, Salix nummularia (C, Dm) 70.3, Solorina crocea (C) 67.9, Lloydia serotina (C) 67.9, Polytrichum piliferum (C) 56.3, Pohlia crudoides 54.6, Gowardia nigricans (C) 53.5*

Constant species: ***Thamnolia vermicularis 100, Sphaerophorus globosus 100, Salix nummularia (Dg, Dm) 100, Ochrolechia frigida 100, Luzula confusa (Dg) 100, Gymnomitrion corallioides (Dg, Dm) 100, Bryocaulon divergens 100, Racomitrium lanuginosum (Dm) 90, Gowardia nigricans (Dg) 90, Pogonatum dentatum (Dg) 80, Oxyria digyna (Dg) 80, Polytrichum strictum 70, Cladonia coccifera s. lat. 70, Polytrichastrum alpinum 60, Pedicularis hirsuta 60, Parmelia omphalodes s. lat. 60, Cladonia uncialis 60, Cladonia gracilis s. lat. 60, Cetraria islandica 60, Alectoria ochroleuca 60,*** *Solorina crocea (Dg) 50, Polytrichum piliferum (Dg) 50, Lloydia serotina (Dg) 50, Hylocomium splendens 50, Dryas octopetala 50, Dicranum elongatum 50*

Dominant species: *Gymnomitrion corallioides (Dg, C) 50, Racomitrium lanuginosum (C) 40, Salix nummularia (Dg, C) 30*

Trends in selected soil and vegetation properties along the summer warmth index (SWI_g) gradient

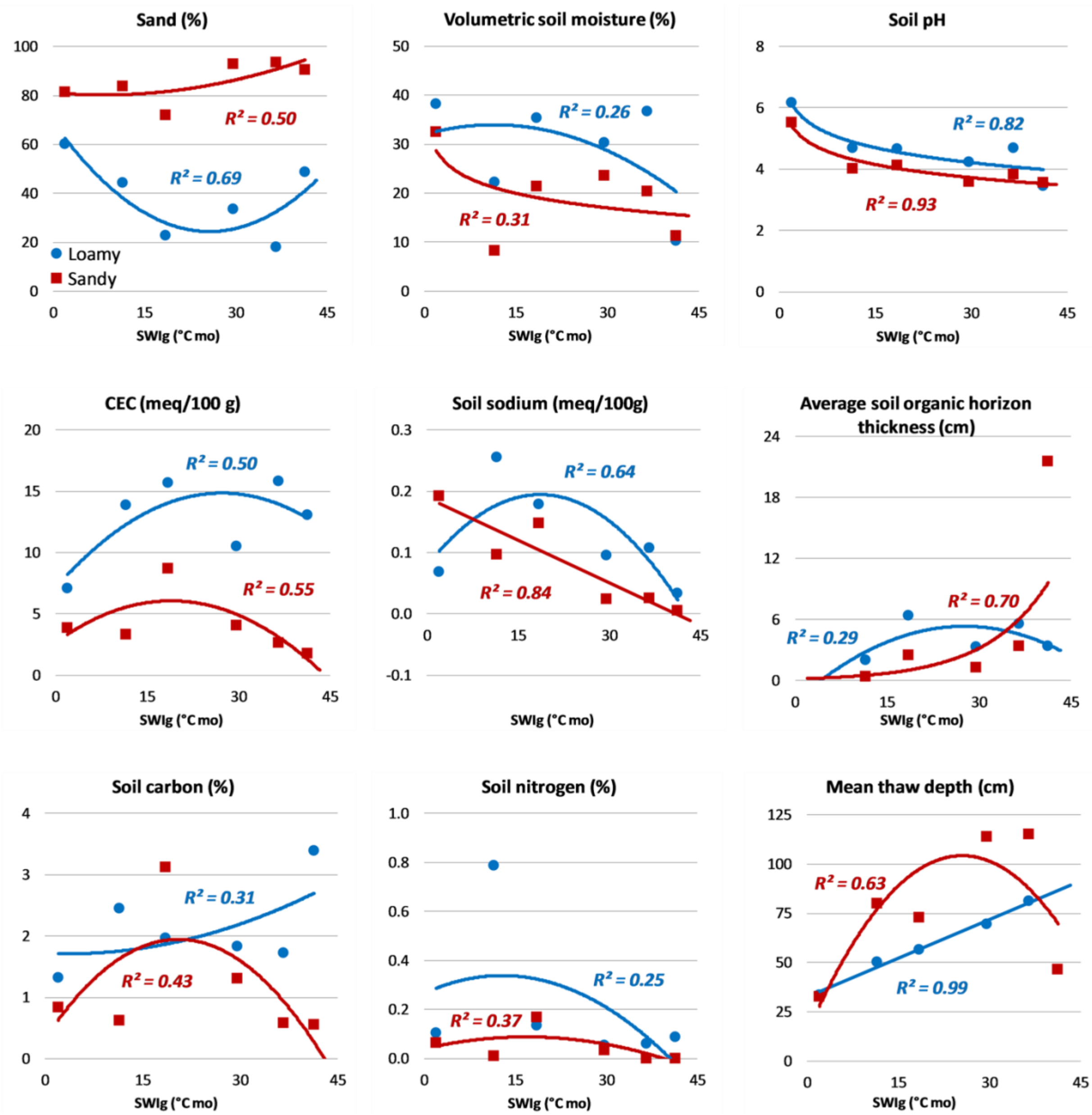

Figure S8.1. Trends in selected soil properties of the top mineral horizon of loamy and sandy sites along the summer-warmth-index (SWI_g) gradient. Variables include percent sand, volumetric soil moisture, soil pH, cation exchange capacity (CEC), soil sodium, thickness of organic soil horizons, percent soil carbon, percent soil nitrogen, and depth of summer thaw at time of measurement. Equations of the trend lines are in Supplemental Information, Appendix S9.

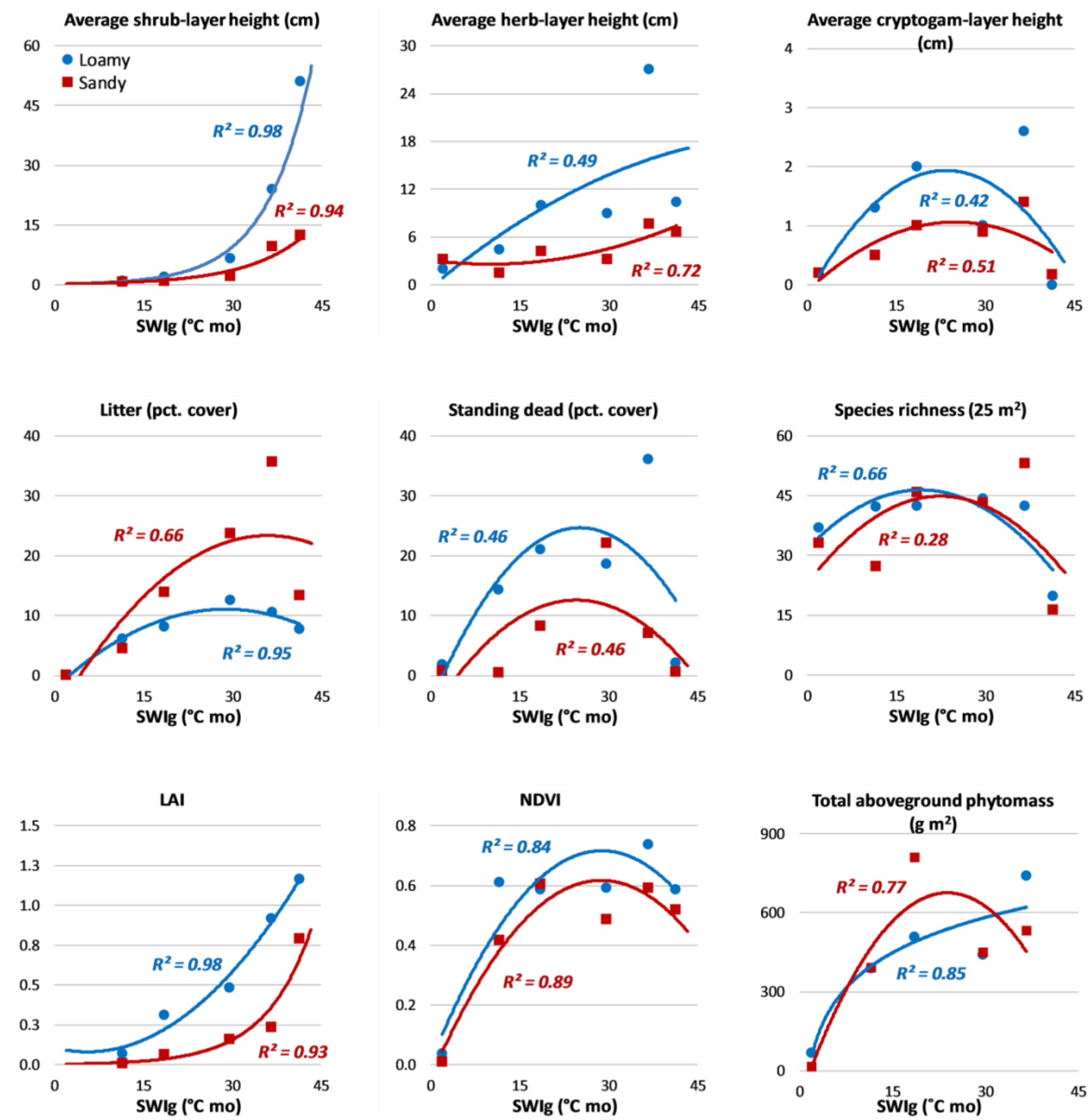

Figure S8.2. Trends of selected vegetation-related factors along the summer-warmth index (SWI_g) gradient on loamy and sandy sites: Shrub-layer height, herb-layer height, moss-layer thickness, live green fraction of total biomass, litter cover, standing dead cover, species richness, leaf area index (LAI), hand-held Normalized Difference Vegetation Index (NDVI). Equations of the trend lines are in Supplemental Information, Appendix S9.

Best-fit regression equations for trend lines of analyzed variables vs. summer warmth index (SWI_g, ˚C mo), loamy and sandy sites along the EAT

Equations are for best-fit trend lines determined in Microsoft Excel.

Variable	Loamy		Sandy	
	Equation	**R^2**	**Equation**	**R^2**
Mean soil textures vs. SWI_g (˚C mo) (Fig. 2)				
Clay	$y = -0.02x^2 + 1.01x + 5.43$	0.28	$y = -0.01x^2 + 0.21x + 2.33$	0.47
Silt	$y = -0.048x^2 + 2.46x + 25.52$	0.80	$y = -0.01x^2 - 0.002x + 16.58$	0.53
Sand	$y = 0.07x^2 - 3.48x + 69.05$	0.69	$y = 0.01x^2 - 0.21x + 81.10$	0.50
Cover (pct.) vs. SWI_g (˚C mo) (Fig. 4a–4c)				
Deciduous shrubs	$y = -0.004x^2 + 1.16x - 0.36$	0.91	$y = -0.06x^2 + 2.88x - 4.57$	0.38
Evergreen shrubs	$y = 0.01x^2 + 0.11x - 0.05$	0.89	$y = 0.01x^2 + 0.32x - 1.23$	0.62
Graminoids	$y = -0.09x^2 + 4.13x - 8.70$	0.93	y = -0.03x2 + 1.49x - 4.53	0.53
Forbs	$y = 0.02x^2 - 1.34x + 17.21$	0.83	$y = 0.05x^2 - 2.76x + 31.39$	0.91
Bryophytes	$y = -0.13x^2 + 5.89x + 1.84$	0.61	$y = -0.08x^2 + 3.35x + 10.19$	0.33
Lichens	$y = 0.18x^2 - 8.80x + 110.23$	0.85	$y = 0.16x^2 - 7.13x + 102.24$	0.67
Mean species richness vs. SWI_g (˚C mo) (Fig. 4d)				
Total species richness	$y = -0.05x^2 + 1.78x + 34.77$	0.69	$y = -0.02x^2 + 1.07x + 30.45$	0.68
Deciduous shrubs	$y = 1.18\ln(x) - 1.18$	0.82	$y = 1.04\ln(x) - 1.18$	0.52
Evergreen shrubs	$y = 0.08x - 0.45$	0.80	$y = 0.09x - 0.28$	0.92
Graminoids	$y = -0.02x^2 + 0.65x - 0.32$	0.95	$y = -0.01x^2 + 0.53x - 0.55$	0.66
Forbs	$y = 0.01x^2 - 0.43x + 8.00$	0.70	$y = 0.005x^2 - 0.35x + 7.56$	0.91
Bryophytes	$y = -0.02x^2 + 0.46x + 13.45$	0.48	$y = 0.002x^2 - 0.02x + 11.20$	0.52
Lichens	$y = -0.03x^2 + 1.10x + 13.25$	0.89	$y = -0.01x^2 + 0.86x + 12.00$	0.82
Soil factors vs. SWI_g (˚C mo) (Supplemental Information, Appendix S8, Fig. S8.1)				
Sand (%)	$y = 0.07x^2 - 3.48x + 69.07$	0.69	$y = 0.01x^2 - 0.22x + 81.12$	0.50
Volumetric soil moisture (%)	$y = -0.02x^2 + 0.35x + 31.95$	0.26	$y = -4.30\ln(x) + 31.63$	0.31
Soil pH	$y = -0.70\ln(x) + 6.60$	0.82	$y = -0.62\ln(x) + 5.83$	0.93
CEC (meq/100 g)	$y = -0.01x^2 + 0.57x + 7.12$	0.50	$y = -0.01x^2 + 0.36x + 2.66$	0.55
Soil sodium (meq/100g)	$y = -0.0003x^2 + 0.01x + 0.08$	0.64	$y = -0.005x + 0.19$	0.84
Average soil organic horizon thickness (cm)	$y = -0.01x^2 + 0.54x - 2.07$	0.29	$y = 0.17e^{0.10x}$	0.70
Soil carbon (%)	$y = 0.001x^2 - 0.005x + 1.72$	0.31	$y = -0.004x^2 + 0.16x + 0.33$	0.43
Soil nitrogen (%)	$y = -0.0004x^2 + 0.01x + 0.27$	0.25	$y = -0.0002x^2 + 0.01x + 0.04$	0.37
Mean thaw depth (cm)	$y = 1.31x + 32.51$	0.99	$y = -0.14x^2 + 7.06x + 14.20$	0.63
Vegetation factors vs. SWIg (˚C mo) (Supplemental Information, Appendix S8, Fig. S8.2)				
Average shrub-layer height	$y = 0.19e^{0.13x}$	0.98	$y = 0.18e^{0.10x}$	0.94
Average herb-layer height	$y = -0.01x^2 + 0.63x - 0.34$	0.49	$y = 0.00x^2 - 0.10x + 3.07$	0.72
Average cryptogam-layer height	$y = -0.00x^2 + 0.18x - 0.20$	0.42	$y = -0.00x^2 + 0.09x - 0.11$	0.51
Litter (pct. cover)	$y = -0.02x^2 + 0.92x - 2.20$	0.95	$y = -0.02x^2 + 1.68x - 6.74$	0.66
Standing dead (pct. cover)	$y = -0.05x^2 + 2.33x - 4.61$	0.46	$y = -0.03x^2 + 1.54x - 6.36$	0.46
Species richness (25 m^2)	$y = -0.04x^2 + 1.55x + 31.66$	0.66	$y = -0.04x^2 + 1.97x + 22.85$	0.28
LAI	$y = 0.001x^2 - 0.01x + 0.11$	0.98	$y = 0.003e^{0.13x}$	0.93
NDVI	$y = -0.001x^2 + 0.05x + 0.01$	0.84	$y = -0.001x^2 + 0.05x - 0.04$	0.89
Total aboveground phytomass (g m^2)	$y = 193.79\ln(x) - 76.71$	0.85	$y = -1.38x^2 + 65.72x - 108.24$	0.77

Mean number of species per plot, summarized by site, soil texture, and major plant-growth-form groups along the Eurasia Arctic Transect

For most sites the mean species richness is based on five 5 x 5-m (25 m^2) plots. VD-1,2 had two loamy sites, and the mean species richness is based on ten 5 x 5-m plots. ND-2 had three 1 x 1-m hummock plots, and 3 1 x 1-m inter-hummock plots. To obtain a somewhat comparable sized area for comparison, species richness at ND-2 was calculated as the total number of unique species encountered in all six 1 x 1-m plots (6 m^2).

Site number	KR-1	BO-1	KH-1	VD-1,2	LA-1	ND-1	KR-2	BO-2	KH-2	VD-3	LA-2	ND-2
Number of plots	5	5	5	10	5	5	5	5	5	5	5	1
Summer warmth index	2.0	11.5	18.5	29.6	36.6	41.3	2.0	11.5	18.5	29.6	36.6	41.3
Bioclimate subzone	A	B	C	D	E	FT	A	B	C	D	E	FT
Soil texture	loamy	loamy	loamy	loamy	loamy	loamy	sandy	sandy	sandy	sandy	sandy	sandy
Lichens	15.2	23.4	21.4	19.4	17.0	6.2	14.4	19.0	22.2	24.6	26.8	20.0
Bryophytes	12.4	23.6	10.2	12.0	13.0	3.0	10.6	12.0	12.0	10.8	12.4	14.0
Graminoids	1.0	5.4	5.8	6.0	4.0	0.2	1.0	2.2	7.0	4.0	4.6	1.0
Forbs	8.2	1.6	3.2	1.4	2.8	0.2	7.0	3.8	2.8	0.4	2.0	0.0
Evergreen shrubs	0.0	1.0	0.2	1.7	2.2	3.8	0.0	1.2	0.8	2.4	2.8	4.0
Deciduous shrubs	0.0	1.0	1.6	3.7	3.4	3.0	0.0	1.0	1.0	1.0	4.4	3.0
Trees	0.0	0.0	0.0		0.0	3.4	0.0	0.0	0.0	0.0	0.0	0.0
Mean total species per plot	36.8	56.0	42.4	44.2	42.4	19.8	33.0	39.2	45.8	43.2	53.0	42.0

Intraset correlation coefficients between four axes of the DCA ordination and tested environmental variables

Coefficients are species-environment correlations, which measure the strength of the relationship between species or environmental variables and the ordination axes in the program CONOCO, which was used for the DCA analysis via JUICE.

Expl Ax1	1													
Expl Ax2	0.1549	1												
Expl Ax3	0.0006	-0.0507	1											
Expl Ax4	0.0847	-0.2418	0.2178	1										
ELEV	-0.1735	-0.1239	-0.0163	-0.2228	1									
MICRORLF	-0.4085	-0.0986	0.2855	-0.1293	0.4592	1								
THAW_DEP	-0.572	0.3622	-0.0812	-0.4036	0.2749	0.6013	1							
SOIL_MOI	0.1054	-0.8775	-0.1302	0.044	0.1771	-0.1041	-0.539	1						
SNOW_DUR	-0.0342	-0.4383	0.7361	0.043	-0.0098	0.2526	-0.111	0.2148	1					
SWI	-0.7742	-0.0403	0.1425	0.0133	0.5721	0.5997	0.728	-0.2509	0.1039	1				
SAND(%)	0.1638	0.7489	0.021	-0.3403	-0.1275	-0.2667	0.3302	-0.6097	-0.4072	-0.0512	1			
CLAY(%)	-0.1895	-0.4958	0.3005	0.128	0.1423	0.3854	-0.2195	0.3829	0.5956	0.1006	-0.8051	1		
Latitude	0.9595	0.1022	-0.0296	0.1314	-0.4014	-0.5264	-0.6893	0.1488	-0.0386	-0.9085	0.1032	-0.1611	1	
AgeTerac	-0.2494	-0.5939	-0.4808	0.271	0.2526	0.1143	-0.0656	0.4106	-0.0596	0.2563	-0.6914	0.318	-0.2414	1
	Expl Ax1	**Expl Ax2**	**Expl Ax3**	**Expl Ax4**	**ELEV**	**MICRORLF**	**THAW_DEP**	**SOIL_MOI**	**SNOW_DUR**	**SWI**	**SAND(%)**	**CLAY(%)**	**Latitude**	**AgeTerac**

Photos of lichen-rich tundra of Hayes Island

Lichen-rich tundra of Hayes Island. The rich lichen cover is able to develop in the cold wet arctic maritime climate and thrives because of the lack of competition from other growth forms and the lack of reindeer on the island. The brown lichens are mainly *Cetrariella delisei* and *Cetraria islandica*. The dominant white lichens are *Stereocaulon alpinum* and *Thamnolia subuliformis*. The yellowish lichens are mainly *Flavocetraria cucullata*. These communities were discovered on the last day of the 2010 expedition and unfortunately were not sampled. Photos: D.A. Walker